Available online at www.sciencedirect.com

ScienceDirect

Journal of Economic Theory 163 (2016) 525–556

JOURNAL OF Economic Theory

www.elsevier.com/locate/jet

Revisiting the model of credit cycles with Good and Bad projects ☆

Kiminori Matsuyama [a,*], Iryna Sushko [b,c], Laura Gardini [d]

[a] *Northwestern University, USA*
[b] *Institute of Mathematics, National Academy of Science of Ukraine, Ukraine*
[c] *Kyiv School of Economics, Ukraine*
[d] *University of Urbino, Italy*

Received 17 August 2015; final version received 23 December 2015; accepted 19 February 2016

Available online 26 February 2016

Abstract

We revisit the model of endogenous credit cycles by Matsuyama (2013, Sections 2–4). First, we show that the same dynamical system that generates the equilibrium trajectory is obtained under a much simpler setting. Such a streamlined presentation should help to highlight the mechanism through which financial frictions cause instability and recurrent fluctuations. Then, we discuss the nature of fluctuations in greater detail when the final goods production function is Cobb–Douglas. For example, the unique steady state possesses *corridor stability* (locally stable but globally unstable) for empirically relevant parameter values. This also means that, when a parameter change causes the steady state to lose its local stability, its effects are *catastrophic* and *irreversible* so that even a small, temporary change in the financial friction could have large, permanent effects on volatility. Other features of the dynamics include *an immediate* transition from the stable steady state to a stable *asymmetric cycle* of period $n \geq 3$, along which $n - 1 \geq 2$ consecutive periods of gradual expansion are followed by one period of sharp downturn, as well as to *a*

☆ This project has evolved from K. Matsuyama's keynote speech at Nonlinear Economic Dynamics Conference, Siena, Italy, July 4–6, 2013 (NED 2013), dedicated to the memory of Richard Goodwin in the centennial of his birth. We thank the organizers and participants of NED 2013, as well as the seminar participants at Keio, JDB-RICF and CREI/Pompeu Fabra for their feedback. K. Matsuyama is grateful to Jess Benhabib for many valuable discussions during his visit to NYU. The work of I. Sushko and L. Gardini has been supported by the COST Action IS1104. The detailed comments by the Co-Editor and the two referees have greatly improved the paper. The usual disclaimer applies.

* Corresponding author.
E-mail addresses: k-matsuyama@northwestern.edu (K. Matsuyama), sushko@imath.kiev.ua (I. Sushko), laura.gardini@uniurb.it (L. Gardini).

http://dx.doi.org/10.1016/j.jet.2016.02.010

robust chaotic attractor. These results demonstrate the power of the skew-tent map as a tool for analyzing a regime-switching dynamic economic model.

JEL classification: C61; E32; E44

Keywords: Composition of credit flows; Financial instability; Corridor stability; The skew-tent map; Regime-switching; Piecewise smooth nonlinear dynamical system

1. Introduction

The idea that market mechanisms are fundamentally unstable is not new. Indeed, the earliest mathematical models of business cycles, those proposed by Hicks, Kaldor, Kalecki, Goodwin, etc., may be viewed as attempts to capture such an idea. Recent events have also renewed interest in the Kindleberger–Minsky hypothesis that financial frictions can be a source of macroeconomic instability and volatility. Yet, following the seminal work of Bernanke and Gertler (1989) and Kiyotaki and Moore (1997), a vast majority of macroeconomic research on financial frictions study propagation mechanisms of exogenous shocks in the presence of financial frictions, within a theoretical setting that ensures the stability of the steady state. Nevertheless, there exist some micro-founded, intertemporal general equilibrium models, in which financial frictions are responsible for making the unique steady state unstable, thereby creating persistent volatility without exogenous shocks; see, e.g., Aghion et al. (1999), Azariadis and Smith (1998), Matsuyama (2007, 2008, 2013) and Myerson (2012, 2014).[1]

The present paper builds on one such model developed by Matsuyama (2013, Sections 2–4), which generates endogenous fluctuations of borrower net worth and aggregate investment. This model considers an overlapping-generations economy in which entrepreneurs arrive sequentially with their endowments of inputs, which are used to produce the final good. Upon arrival, they first sell their endowments of inputs to acquire some net worth that is used later to finance their own projects or to lend to finance the projects run by others. There are two types of investment projects, *the Good* and *the Bad*. The Good projects generate capital, which produces the final good using inputs supplied by the next generations of entrepreneurs who might undertake projects of their own. By competing for these inputs, more Good projects drive up the price of these inputs, thereby improving the net worth of next generations of entrepreneurs. In contrast, the Bad projects are independently profitable as they directly generate the final good. Without generating demand for any inputs, these projects do not improve the net worth of next generations of entrepreneurs. Furthermore, the Bad projects are subject to borrowing constraints due to the limited pledgeability of their revenue so that the entrepreneurs need to have enough net worth of their own to finance them. The unique equilibrium path of this economy, governed by a one-dimensional nonlinear piecewise smooth map, may fluctuate persistently for almost all initial conditions. With a low net worth, all the credit flows to finance the Good, even when the Bad

[1] See also Favara (2012), Figueroa and Leukhina (2013), Martin (2008), and Reichlin and Siconolfi (2004). There is also a literature on dynamic models of financial frictions that generate multiple equilibrium trajectories, some of which exhibit "expectations-driven" fluctuations. In these models, such fluctuating equilibrium trajectories co-exist with an equilibrium trajectory that does not fluctuate. In contrast, the models cited here generate fluctuations along the unique equilibrium trajectory for almost all initial conditions.

projects are more profitable than the Good projects. This over-investment to the Good creates a boom, which generates pecuniary externalities to the next generation of the entrepreneurs by improving their net worth. With their net worth improved, these entrepreneurs are able to finance the Bad projects. Credit flows are redirected from the Good to the Bad. This change in the composition of credit flows at the peak of the boom causes a deterioration of borrower net worth. The whole process repeats itself. The equilibrium path oscillates, as the Good breed the Bad and the Bad destroy the Good. Such instability and persistent volatility occur whenever the Bad projects are sufficiently profitable but come with an intermediate degree of pledgeability. This implies, among other things, that an improvement in the financial system could lead more volatility.

Note that this model shares the same observation with a vast majority of macroeconomic research of financial frictions that started with Bernanke and Gertler (1989). That is, in the presence of financial frictions, saving does not necessarily flow into the most profitable investment projects, and this problem can be alleviated (aggravated) by a higher (lower) borrower net worth. What separates this model from the majority of the literature is the assumption on the set of profitable investment projects that compete for credit. In the Bernanke and Gertler model, for example, all the profitable investments contribute equally to improve net worth of other borrowers and the only alternative use of saving, storage, is unprofitable, subject to no borrowing constraint, and generates no pecuniary externalities to the next generation of entrepreneurs. This means that, when an improved net worth allows more saving to flow into the profitable investments, saving is redirected *towards* the investments that generate pecuniary externalities, which further improve borrower net worth. This mechanism thus generates *persistence* of a low borrower net worth, causing a slow recovery and prolonged recessions in their model (and many others in the literature). The model with Good and Bad projects differs from Bernanke and Gertler and others in that *not all* the profitable investments have the same demand spillover effects. *Some* profitable investments, which are subject to the borrowing constraints, do not improve the net worth of other borrowers. This means that, when an improved net worth allows more saving to flow into such profitable investments, saving may be redirected *away from* the investments that generate pecuniary externalities, which causes a deterioration of borrower net worth. This is the mechanism behind macroeconomic instability, and volatility.[2]

This mechanism, – an easy credit extended to the Bad projects during the boom can be responsible for a subsequent bust –, captures the popular idea, "successes breed crises." And it is consistent with the evidence of "credit booms gone bust," found by Mendoza and Terrones (2008) and Schularick and Taylor (2012) and many others, showing that credit growth is the best

[2] Needless to say, the two mechanisms, the one implying *persistence* and the other *volatility*, are not mutually exclusive and can be usefully combined. Indeed, Matsuyama (2013, section 5) presented a hybrid model, which allows for three types of projects, *the Good*, *the Bad*, and *the Ugly*. Only the Good improve the net worth of other borrowers; neither the Bad nor the Ugly improve net worth of other borrowers. The Bad are profitable but subject to the borrowing constraint. The Ugly are unprofitable but subject to no borrowing constraint (as storage in the Bernanke–Gertler model). Thus, when the net worth is low, the Good compete with the Ugly, which act as a drag on the Good, thereby adding persistence in the macro dynamics. When the net worth is high, the Good compete with the Bad, which destroy the Good, causing instability and volatility. By combining the two effects, this hybrid model generates *intermittency* phenomena. That is to say, relatively long periods of small and persistent movements are punctuated intermittently by seemingly random-looking behaviors. Along these cycles, the economy exhibits *asymmetric fluctuations*; it experiences a slow process of recovery from a recession, followed by a rapid expansion, and, possibly after a period of high volatility, plunges into a recession. This extension also serves another purpose. It demonstrates that we do not need to assume that more productive projects with tighter borrowing constraints to have less demand spillovers on average. What is needed for instability and endogenous volatility is that *some* productive projects with less spillovers can be financed only at a higher level of borrower net worth.

predictor of the likelihood of a financial crisis. In fact, it resembles the financial instability hypothesis of Kindleberger (1996) and Minsky (1982), which also emphasizes that an economic expansion often comes to an end due to the changing nature of credit and investment at the peak of the boom. Kindleberger (1996; Appendix B) offered a catalogue of financial boom-and-busts in history, with a long list of investments, such as precious metals, foreign bonds, new technology stocks, real estate and many others, that attracted the attention of investors at the peak of each boom and triggered the crisis that followed. According to Kindleberger and Minsky, this occurs because, after the periods of expansion, people become more driven by "euphoria," "greed," and "manias," which causes more credit to be extended to finance some activities of "dubious" characters. The model with Good and Bad projects, in contrast, does not rely on any form of irrationality. Instead, a higher borrower net worth at the peak of a boom enables projects with less pecuniary externalities to compete for credit, thereby diverting credit away from projects with more pecuniary externalities, which make it impossible to sustain the boom. In this regard, it is more similar in spirit to recent studies by Favara (2012), Figueroa and Leukhina (2013), Martin (2008), and Reichlin and Siconolfi (2004), which also generate recurrent volatility through endogenously changing composition of credit in fully specified intertemporal general equilibrium models without relying on the irrationality of agents.

Our contribution in this paper is twofold. First, we reformulate the model of Matsuyama (2013, Sections 2–4) and show that the same, one-dimensional nonlinear piecewise smooth map that governs the equilibrium trajectory of the economy, can be derived under a much simpler setting. Such a streamlined presentation should help to highlight the key mechanism that causes instability and recurrent fluctuations in the model of Good and Bad projects, by focusing on the essentials.[3]

Second, we discuss in detail the nature of fluctuations under the additional assumption that the production function of the final good sector is Cobb–Douglas. With this assumption, the map has four parameters, the share of capital in the Cobb–Douglas production function (α), the fixed investment size of the Bad projects (m), the rate of return of the Bad projects (B); and the pledgeability of the Bad projects (μ). In fact, when the Bad projects are sufficiently profitable (i.e., for a sufficiently high B), the last two enter the equation only through their product, μB, the pledgeable rate of return of the Bad projects, so that the map has only three parameters, α, m, and μB. We characterize the dynamics in terms of these parameters. To summarize our findings,

i) For fixed values of α and m, the unique steady state is unstable and the equilibrium trajectory exhibits permanent fluctuations for almost all initial conditions for an intermediate range of μB.
ii) As μB enters this instability range from above the unique steady state loses its local stability via a *subcritical flip bifurcation* for empirically relevant values of $\alpha < 0.5$.[4] Before such a subcritical flip, the (locally) stable steady state co-exists with a stable period-2 cycle, along

[3] Remark 2 below explains the differences between the original and present formulations of the model in detail. The original formulation in Matsuyama (2013) has many additional ingredients, which are included mostly to demonstrate the robustness of the mechanism and to clarify the assumptions that are essential from those that are merely simplifying. While useful, it has a drawback of obscuring the mechanism.

[4] In the language of the dynamical system theory, a *bifurcation* occurs when an infinitesimal change in the parameter values of a system causes a qualitative (topological) change in its properties. Bifurcations may be classified according to the types of qualitative changes caused. *Subcritical flip* is one particular type of bifurcation. *Border-collision* is another. Their main economic implications are explained briefly in the remainder of this paragraph and in detail in Section 4.2.

with an unstable period-2 cycle, whose *stable set* separates their *basins of attraction*.[5] This implies *corridor stability*, to use the terminology of Leijonhufvud (1973). That is, the steady state of the economy is locally stable but globally unstable so that it is self-correcting against small shocks but not against large ones.[6] Furthermore, when the steady state loses its local stability via a subcritical flip, the effects are *catastrophic* and *irreversible*. This suggests, among other things, that a temporary credit crunch shock, captured by a one-time reduction in the pledgeability parameter, would have a permanent effect on the volatility of the economy.

iii) As μB enters this instability range from below the unique steady state loses its local stability via a *border collision bifurcation*. After this bifurcation, this dynamics is characterized by one of the following three types of asymptotic behaviors, depending on the parameter values; i) a stable cycle of period 2; ii) a stable *asymmetric cycle* of period $n \geq 3$, along which the economy experiences $n-1 \geq 2$ consecutive periods of gradual expansion, followed by one period of sharp downturn,[7] or iii) *a robust chaotic attractor*.

Perhaps the significance of the findings listed under iii) needs to be elaborated. Many existing examples of chaos in economics are *not* attracting, particularly those relying on the Li–Yorke theorem of "period-3 implies chaos." This theorem states that, on the system defined by a continuous map on the interval, the existence of a period-3 cycle implies the existence of a period-n cycle for any $n \geq 2$, as well as the existence of an aperiodic (chaotic) trajectory. However, the trajectory can be chaotic only for a set of initial conditions that is of measure zero. For chaos to be observable, it has to be attracting, so that at least a positive measure of initial conditions would converge to it. Furthermore, most existing examples of chaotic attractors in economics are *not* robust (i.e., they do *not* exist for an open region of the parameter space), because the set of parameter values for which a stable cycle exists is dense, and the set of parameter values for which a chaotic attractor exists is totally disconnected (although it may have a positive measure). Moreover, a transition from the stable steady state to chaos often requires an infinite cascade of bifurcations, as these are general features of a system generated by everywhere smooth maps, which most applications assume.[8] In contrast, the present model generates a robust chaotic attractor and a transition from the stable steady state to a stable cycle n-cycle ($n \geq 3$) or to a robust chaotic attractor can be immediate, because it is a "regime-switching" model, characterized by a piecewise smooth system.

[5] In the language of the dynamical system theory, the set of initial conditions that converge to an attractor (that is, an attracting invariant set, such as an attracting steady state, an attracting period-2 cycle, a chaotic attractor, etc.) is called its *basin of attraction*, and the set of initial conditions that converge to an invariant set, which is not necessarily attracting (such as an unstable steady state, an unstable period-2 cycle, etc.) is called its *stable set*.

[6] While many economists are aware of the possibility that nonlinear dynamic models could generate endogenous fluctuations in the absence of exogenous shocks, very few seem to be aware that corridor stability is another implication of nonlinearity; see Benhabib and Miyao (1981) for a valuable exception. Our demonstration of corridor stability should at least provide the reader with a caution against the common practice of studying dynamic models by linearizing around the steady state.

[7] Confusions sometimes occur as the word "period" is used differently in the dynamical system theory. In their language, "period" means the duration of a cycle. That is, "a period-n cycle" or "an n-cycle," is defined as "a cycle whose period is n," or "a cycle that repeats itself every n-th iteration." In this paper, we use "period" as a unit of time, following the common usage of this word in economics. Thus, "a period-n cycle" or "an n-cycle" can be defined as "a cycle whose duration is n periods," or "a cycle that repeats itself every n-th period".

[8] In an early survey on chaos in economics, Baumol and Benhabib (1989, see p. 97) discussed these limitations of smooth dynamical systems. Yet, the message seems to have been lost among the economics profession.

We are able to show these findings thanks to recent advances in the theory of piecewise smooth dynamical systems, which have many properties that are quite distinct from (and in many ways, much simpler than) those defined by smooth (that is, C^∞, such as polynomial) maps. These mathematical tools should find wide applications, given that many dynamic macro models of financial frictions are regime-switching, which naturally make the system piecewise smooth. In particular, it should be relatively easy to obtain in many regime-switching models something analogous to our results summarized in iii) above, because they rely only on the fact that, when the unique steady state of a unimodal map is sufficiently close to its kinked peak, it can be approximated by a piecewise linear map, called the skew-tent map, for which a complete analytical characterization is available. Needless to say, a rigorous treatment of these materials is beyond the scope of this paper, as it requires substantial prior knowledge of the dynamical system theory. Nevertheless, we hope that our non-technical, heuristic exposition and "cookbook" presentation of how to use it, written in the economist friendly language, serves as a useful introduction to this branch of mathematics for the economics audience.[9]

The rest of the paper is organized as follows. Section 2 offers a reformulation of the endogenous credit cycles model with Good and Bad projects, and derives the dynamical system that generates the equilibrium trajectory. Section 3 offers the typology of the dynamic behaviors for the general case, and a preliminary bifurcation analysis. Section 4 provides a more detailed bifurcation analysis for the Cobb–Douglas case. We also look at the transient behaviors of this system numerically. Section 5 concludes.

2. Reformulating the model of credit cycles with good and bad projects

Time is discrete and extends from zero to infinity ($t = 0, 1, 2, \ldots$). The basic framework used is the Diamond (1965) overlapping generations model with two period lives. There is one final good, the *numeraire*, which can be either consumed or used as inputs into investment projects. The final goods sector uses constant returns to scale technology, $Y_t = F(K_t, L_t)$, where K_t is physical capital and L_t is labor. Let $y_t \equiv Y_t/L_t = F(K_t/L_t, 1) \equiv f(k_t)$, where $f(k_t)$ satisfies $f'(k) > 0 > f''(k)$, $f(0) = 0$ and $f'(0) = \infty$. For simplicity, physical capital is assumed to depreciate fully in one period. The factor markets are competitive and thus the factor rewards for physical capital and for labor are equal to $\rho_{t+1} = f'(k_{t+1})$, which is decreasing in k_{t+1}, and $w_t = f(k_t) - k_t f'(k_t) \equiv W(k_t) > 0$, which is increasing in k_t.

At the beginning of each period, a unit measure of homogeneous agents arrives and stays active for two periods. During the first period (when they are "young"), each agent supplies inelastically one unit of labor to the final goods sector to earn $w_t = W(k_t)$, so that $L_t = 1$. They consume only during the second period (when they are "old"). Thus, the young agents save all of the earnings, hence $w_t = W(k_t)$ is also equal to their net worth at the end of period t, as well as the aggregate supply of the credit in the economy.

At the end of their first period, the agents allocate the net worth to maximize their consumption in their second period. In addition to lending to the other agents in the same cohort at the gross rate of return, r_{t+1}, they have access to two types of investment projects; the *Good* and the *Bad*. The Good projects convert one unit of the final good at the end of period t into one unit of physical capital, which becomes available and used in the final goods sector in period $t + 1$.

[9] For an overview of the theory of dynamical systems defined by piecewise smooth one-dimensional maps, see Avrutin et al. (2015). Sushko et al. (2015) provides a detailed analysis of the skew-tent map. Gardini et al. (2008) applies the skew-tent map to characterize the growth cycle model of Matsuyama (1999).

Thus, the gross rate of return of this project is equal to $\rho_{t+1} = f'(k_{t+1})$. The Bad projects are indivisible, and each agent can run at most one Bad project, which transforms $m > 0$ units of the final good in period t into mB units of the final good in period $t+1$, where B is the profitability of the Bad projects. Due to the fixed investment size, $m > 0$, each agent who wants to run this project needs to borrow $m - w_t > 0$ at the rate equal to r_{t+1}. (We will later impose the parameter restrictions to ensure that $w_t < m$ holds along the equilibrium path.)

The agents always have options of lending to the others at r_{t+1} and of investing into the Good projects to earn the rate of return $\rho_{t+1} = f'(k_{t+1})$, which ensures that $r_{t+1} = f'(k_{t+1})$. Some young agents may run the Bad projects. This happens whenever they are both *willing* to run the projects and *able* to finance them. By running Bad projects, they can consume $mB - r_{t+1}(m - w_t) = m(B - r_{t+1}) + r_{t+1}w_t$. By not running Bad projects, they consume $r_{t+1}w_t = f'(k_{t+1})w_t$. Thus, the young agents are *willing* to run the Bad projects if and only if:

$$B \geq r_{t+1} = f'(k_{t+1}). \tag{1}$$

We shall call (1) the *Profitability Constraint* for the Bad projects or simply PC.

Even if PC holds, the agents may not be able to invest in the Bad projects due to the borrowing constraint. The borrowing limit exists because borrowers can pledge only up to a fraction of the project revenue for the repayment, μmB, where $0 < \mu < 1$.[10] Knowing this, the lender would lend only up to $\mu mB/r_{t+1}$. The agents can thus borrow to run the Bad projects if and only if:

$$\mu mB \geq r_{t+1}(m - w_t). \tag{2}$$

We shall call (2) the *Borrowing Constraint* for the Bad projects or simply BC. For some young agents to invest in the Bad projects both BC and PC must be satisfied. Notice that BC is tighter than PC for $w_t < w_\mu \equiv (1-\mu)m$, and PC is tighter than BC for $w_t > w_\mu$.

To characterize the credit market equilibrium, it is useful to define $R(w_t)$, the maximal rate of return that a young agent with the net worth w_t could pledge to the lender by running a Bad project without violating PC and BC. From (1) and (2), it is given by:

$$R(w_t) \equiv B\, Min\left\{\frac{\mu}{1 - w_t/m}, 1\right\} = \begin{cases} \frac{\mu B}{1-w_t/m} & \text{if } w_t \leq w_\mu \\ B & \text{if } w_t \geq w_\mu. \end{cases} \tag{3}$$

The graph of this function is shown both in Fig. 1a and Fig. 2a. For $w_t < w_\mu$, when BC is the relevant constraint, $R(w_t)$ is strictly increasing because a higher net worth eases BC, allowing the agents to credibly pledge a higher rate of return to the lender, when running the Bad projects. For $w_t > w_\mu$, BC is no longer binding, hence $R(w_t)$ is flat at $R(w_t) = B$.

We are now ready to describe the credit market equilibrium. Suppose that $f'(k_{t+1}) = r_{t+1} < R(w_t)$. Then, both PC and BC would be satisfied with strict inequalities, which means that each young agent would be able to borrow and run a Bad project and would be strictly better off by doing so than by lending or investing into the Good projects. Thus, no agent would lend, and hence no agent could borrow, which is a contradiction. Thus, $f'(k_{t+1}) = r_{t+1} \geq R(w_t)$ must hold in equilibrium. If $f'(k_{t+1}) = r_{t+1} > R(w_t)$, then at least PC or BC is violated, so that no

[10] See Tirole (2005) for the pledgeability approach to modeling financial frictions and Matsuyama (2008) for a variety of applications in macroeconomics. They also discuss various stories of agency problems that can be told to justify the assumption that the borrowers can pledge only up to a fraction of the project revenue. Nevertheless, its main appeal is the simplicity, which makes it suitable for studying dynamic general equilibrium implications of financial frictions.

a) All credit flows into the Good for $w_t \equiv W(k_t) < w_B \equiv W(k_B)$, i.e., $f'(w_t) > B$. All additional credit flows into the Bad for $w_t \equiv W(k_t) > w_B \equiv W(k_B)$. Hence, $k_c = k_B$.

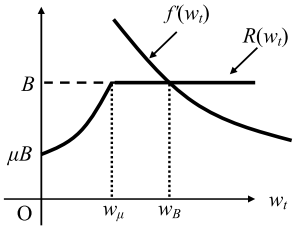

b) The map has two branches with one kink at k_B: upward on the Left and flat on the Right

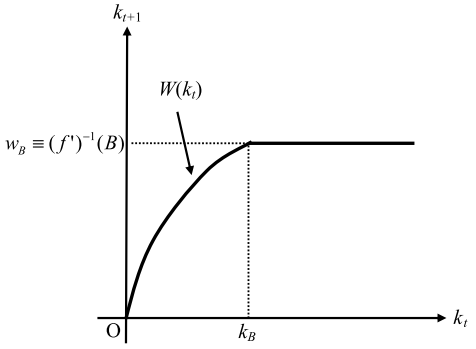

Fig. 1. **Non-distortionary case**: $f'(w_\mu) > B \Leftrightarrow w_\mu \equiv W(k_\mu) < w_B \equiv W(k_B)$.

agents would run the Bad projects. Only when $f'(k_{t+1}) = r_{t+1} = R(w_t)$, some Bad projects are initiated. Therefore,

$$f'(k_{t+1}) \geq R(w_t); \qquad X_t \geq 0; \qquad \left[f'(k_{t+1}) - R(w_t)\right]X_t = 0, \tag{4}$$

where $0 \leq X_t < 1$ denotes the measure of the Bad projects initiated in period t, as well as the measure of young agents running them. (The parameter restrictions that ensure $w_t < m$ also ensures $X_t < 1$, as shown later.) In addition, the condition that the aggregate credit supply equals the aggregate credit demand can be written as:

$$w_t = k_{t+1} + mX_t. \tag{5}$$

The credit market equilibrium at the end of period t is given by k_{t+1} and X_t that solve (4) and (5) for a given $w_t = W(k_t)$.

From (4), we have $f'(k_{t+1}) = R(w_t)$, whenever $X_t > 0$. From (5), $k_{t+1} = w_t$ whenever $X_t = 0$. Thus, using $w_t = W(k_t)$, we obtain the dynamical system in k_t as:

$$k_{t+1} = \Psi(k_t) \equiv \begin{cases} W(k_t) & \text{if } k_t \leq k_c \\ (f')^{-1}(R(W(k_t))) & \text{if } k_t \geq k_c, \end{cases} \tag{6}$$

where k_c is the critical level of k at which the credit starts flowing into the Bad projects and it is defined by $f'(W(k_c)) \equiv R(W(k_c))$.

a) All the credit continues flowing into the Good, even after $f'(w_t) = B$, implying $w_B \equiv W(k_B) < W(k_c) \equiv w_c$. After $w_t \equiv W(k_t) = W(k_c) \equiv w_c$, the credit is diverted away from the Good to the Bad, until $w_t \equiv W(k_t) = W(k_\mu) \equiv w_\mu$, after which all additional credit flows into the Bad.

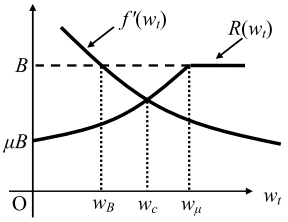

b) The map has three branches with two kinks, $k_c < k_\mu$: upward on the left ($k_t < k_c$), downward in the middle ($k_c < k_t < k_\mu$), and flat on the right ($k_t > k_\mu$). Over-Investment of the Good for ($k_B < k_t < k_\mu$).

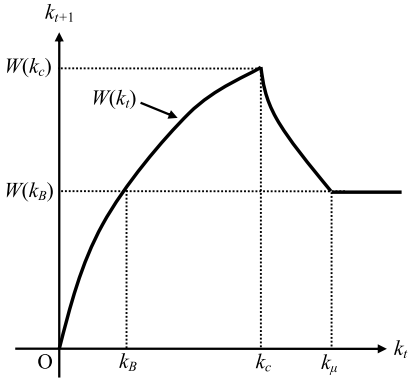

Fig. 2. **Distortionary case**: $f'(w_\mu) < B \Leftrightarrow w_\mu \equiv W(k_\mu) > w_B \equiv W(k_B)$.

We are now ready to define an *equilibrium* of this economy, which is a *sequence*, $\{k_t\}_{t=0}^{\infty}$, that satisfies (6) for an exogenously given $k_0 > 0$. To emphasize that it is a sequence, we often refer to it as an "equilibrium trajectory."[11]

For the remainder of this paper, we assume:

(A1) There exists $\bar{K} > 0$ such that $W(\bar{K}) = \bar{K}$ and $W(k) > k$ for all $k \in (0, \bar{K})$.
(A2) $\bar{K} < m$.

Assumption A1 holds, e.g., for the Cobb–Douglas production, $f(k) = A(k)^\alpha$ with $\alpha \in (0, 1)$. This assumption plays three different roles. First, it rules out an uninteresting case, where the dynamics of k_t would converge to zero in the long run. Second, it implies that, in the absence of the Bad projects, the dynamics $k_{t+1} = \Psi(k_t) = W(k_t)$ would converge monotonically to $\bar{K}$, and hence any fluctuations generated by Eq. (6) could be attributed to the composition of the credit between the Good and the Bad. Third, under A1, $k_t \leq \bar{K}$ implies $k_{t+1} \leq W(k_t) \leq W(\bar{K}) = \bar{K}$, so

[11] In the language of the dynamical system theory, "an equilibrium" means a fixed point of the system, i.e., $k* = \Psi(k*)$ in (6). In this paper, we call it a "steady state," following the standard terminology in economics.

that the dynamical system (6) maps $(0, \bar{K}]$ into itself. Thus, for any initial value, $k_0 \in (0, \bar{K}]$, the equilibrium trajectory of this economy can be obtained by iterating (6), and $W(\bar{K}) = \bar{K}$ can be interpreted as the maximal attainable net worth in this economy. Assumption A2 implies $w_t = W(k_t) \leq W(\bar{K}) = \bar{K} < m$, and hence that the young agents always need to borrow to run the Bad projects, and that only a fraction of the young agents run the Bad projects, $X_t < w_t/m < 1$, as have been assumed.

Non-distortionary case Fig. 1a illustrates the credit market equilibrium for the case where $f'(w_\mu) > B$ or equivalently, $w_\mu < (f')^{-1}(B) \equiv w_B \equiv W(k_B)$. Under this condition, $W(k_c) \equiv w_c = w_B = W(k_B) > w_\mu \equiv W(k_\mu)$, and Eq. (6) can be rewritten as:

$$k_{t+1} = \Psi(k_t) \equiv \begin{cases} \Psi_L(k_t) \equiv W(k_t) & \text{if } k_t \leq k_c = k_B \\ \Psi_R(k_t) \equiv w_B & \text{if } k_t \geq k_c = k_B. \end{cases} \tag{7}$$

As shown in Fig. 1b, the map in Eq. (7) is piecewise smooth with one kink, $k_c = k_B$, which separates an upward-sloping left branch and a flat right branch. On the left branch, $k_t < k_B$, w_t is sufficiently small that the Good are more profitable than the Bad, even if all the credit flows to the Good, $f'(W(k_t)) > B$. Hence all the credit indeed flows to the Good. As k_t increases and more credit flows to the Good, its profitability declines, and at $k_t = k_B$, it becomes as profitable as the Bad, $f'(W(k_B)) \equiv f'(w_B) \equiv B$. At this point, BC is no longer binding because $w_B > w_\mu$. Hence, an additional credit would flow to the Bad, which is why the map is flat, whenever $f'(W(k_t)) < B$, that is, on the right branch, $k_t \geq k_B$. Note that in this case, BC is never binding along the equilibrium path. The aggregate credit is always allocated efficiently, flowing to the most profitable projects, thereby equalizing the profitability of the two projects whenever both attract some credit in equilibrium.

Distortionary case Fig. 2a illustrates the credit market equilibrium for the case where $f'(w_\mu) < B$ or equivalently, $w_\mu > (f')^{-1}(B) \equiv w_B$. Under this condition, $w_B < w_c < w_\mu$ or $k_B < k_c < k_\mu$, and Eq. (6) becomes:

$$k_{t+1} = \Psi(k_t) = \begin{cases} \Psi_L(k_t) \equiv W(k_t) & \text{if } k_t \leq k_c \\ \Psi_M(k_t) \equiv (f')^{-1}\left(\frac{\mu B}{1 - W(k_t)/m}\right) & \text{if } k_c \leq k_t \leq k_\mu \\ \Psi_R(k_t) \equiv w_B & \text{if } k_t \geq k_\mu, \end{cases} \tag{8}$$

where k_c satisfies $f'(W(k_c)) = \frac{\mu B}{1 - W(k_c)/m} < B$. As shown in Fig. 2b, the map is piecewise smooth with two kinks, $k_c < k_\mu$ which separate the following three branches.

- ***L*: Left (upward) branch** $(0 < k_t < k_c)$. All the credit goes to the Good, either because PC fails (when $k_t < k_B$), or because BC fails, even though PC holds with strict inequality (when $k_B < k_t < k_c$). It is upward-sloping because a higher aggregate saving $W(k_t)$ would allow more credit to flow into the Good projects.
- ***M*: Middle (downward) branch** $(k_c < k_t < k_\mu)$. Some credit goes to the Bad, because the net worth becomes high enough that the Bad can compete with the Good. It is downward-sloping, because BC is still binding in this range so that a higher net worth makes it easier to finance the Bad, which bids up the equilibrium rate of return, thereby diverting the credit flows away from the Good.
- ***R*: Right (flat) branch** $(k_\mu < k_t \leq \bar{K})$. The Bad are no longer borrowing-constrained. It is PC that is the binding constraint. Hence, the Good and the Bad are equally profitable. It is

flat because the Good are subject to diminishing returns, so that additional credit would flow into the Bad.

Note that the map has a hump over $k_B < k_t < k_\mu$, in which $f'(k_{t+1}) < B$ holds. In this range, the Bad projects satisfy PC with strict inequality, implying an overinvestment to the Good. Although all young agents are eager to run the Bad projects, some of them are unable to do so due to BC. For $k_B < k_t < k_c$, BC cannot be satisfied, hence $X_t = 0$ and no credit flows into the Bad. For $k_c < k_t < k_\mu$, BC holds so that $X_t > 0$ and some credit flows to the Bad, but BC is the binding constraint, causing an overinvestment to the Good (and an underinvestment to the Bad).

This completes the description of the model. Before proceeding to characterize the dynamics, a few remarks are in order. Those eager to see the characterization of the dynamics may want to skip them at first reading.

Remark 1. In this model, only a fraction of the young agents run the Bad projects, when $r_{t+1} = R(W(k_t))$ holds (i.e., in $\boldsymbol{M}$ and $\boldsymbol{R}$). In $\boldsymbol{R}$, $r_{t+1} = R(W(k_t)) = B$ and PC is satisfied with equality. Thus, some young agents run the Bad projects while others do not, simply because they are indifferent. In $\boldsymbol{M}$, $r_{t+1} = R(W(k_t)) < B$, and BC is binding but PC is satisfied with strict inequality. In other words, all the young agents strictly prefer borrowing to run the Bad projects over lending their net worth to others. Thus, the equilibrium allocation necessarily involves credit rationing, where some of the young are denied credit. Those who denied credit cannot entice the potential lenders by promising a higher rate of return, because the lenders would know that the borrowers would not be able to keep the promise. It should be noted, however, that equilibrium credit rationing occurs in this model due to the homogeneity of the agents. It is possible to extend the model to eliminate the credit rationing without changing the essential features of the model. For example, suppose that the labor endowment of the agents is given by $1 + \varepsilon z$, where ε is a small positive number and z is distributed with the mean equal to zero, with no mass point and a bounded support. Then, the allocation of the credit in period t is determined by a critical value, z_t, i.e., the agents, whose endowments are greater than or equal to $1 + \varepsilon z_t$ obtain the credit and run the Bad projects, and those whose endowments are less than $1 + \varepsilon z_t$ becomes the lenders. The model above can be viewed as the limit case, where ε goes to zero. What is essential for the analysis is that, when the borrowing constraint is binding for the marginal agents, a higher w_t eases the borrowing constraint, which lowers the critical value, z_t, allowing more agents to finance the Bad projects, which drive up r_{t+1}. Thus, it is the borrowing constraint, not the equilibrium credit rationing per se, that matters. The equilibrium credit rationing is nothing but an artifact of the homogeneity assumption, which is imposed to simplify the analysis.

Remark 2. The model presented here differs in several ways from the one presented in Section 2 of Matsuyama (2013). In that model, both the Good and the Bad are indivisible and subject to the borrowing constraints. The agents are not homogeneous; instead there are three types of agents, "the entrepreneurs," "the traders," and 'the lenders". Each entrepreneur has access to a Good project, which consists of paying the fixed cost to set up a firm when young and running it when old, which requires hiring some young agents as workers.[12] Each trader has access to a Bad

[12] Setting up a firm allows each entrepreneur to produce the final good with $y = \varphi(\ell)$, with $\varphi'(\ell) > 0 > \varphi''(\ell)$, where ℓ is the number of workers per firm. By measuring capital by the equilibrium number of firms (also the measure of entrepreneurs undertaking the Good projects), the capital/labor ratio is $k = 1/\ell$ and the final goods production per worker is $f(k) = k\varphi(1/k)$.

project, which consists of hoarding or storing the final good for one period, without generating any demand for labor endowment held by the next generation of the agents. The lenders have access to neither the Good nor the Bad. These additional elements were introduced in part to help the narrative, in part to demonstrate the robustness of the key results, and in part to facilitate one of the extensions in that paper, which introduces a third type of projects, the Ugly.[13] However, these are not essential elements of the mechanism that generates instability and fluctuations in that model. The present model offers a simpler presentation of the mechanism by removing all these complications.

Remark 3. As explained in Matsuyama (2013), the terminology, the Good and the Bad, reflects differential propensity to generate pecuniary externalities; the Good improve the net worth of future borrowers but the Bad do not. Hence, shifting the composition of the credit towards the Bad is bad for the next generations of the borrowers.[14] Here, this key feature is introduced by assuming that the Good rely on the "labor" supplied by the next generation, while the Bad are independently profitable. "Labor" should not be literally interpreted. Instead it should be interpreted more broadly to include any inputs supplied or any assets held by potential future borrowers, who could sell them or use them as collaterals to ease their borrowing constraints. Beyond such differential general equilibrium prices effects, the mechanism does not require what these projects must be like. In more general settings, the projects that generate more pecuniary externalities than others need not be more "productive" or more "labor-intensive." Furthermore, the other differences between the two – the Bad are indivisible and subject to the borrowing constraint, while the Good are not –, are not essential, as has been demonstrated in Matsuyama (2013).

3. Dynamic analysis: general case

First, note that our dynamical system, (6), has a unique steady state, $k^* \in (0, \bar{K}]$. Depending on whether it is located in $\boldsymbol{L}$, $\boldsymbol{M}$, or $\boldsymbol{R}$, we denote it by k_L^*, k_M^* or k_R^*. Fig. 3 offers a classification of this dynamical system in the parameter space, (μ, B), for a given $m \in (\bar{K}, f(\bar{K}))$. What separates these cases, illustrated by Figs. 4a–4e, is the relative magnitude of four critical values of $k : k_B$ (the point at which the Bad become as profitable as the Good if all the credit goes to the Good), k_c (the point at which the Bad start attracting the credit), k_μ (the point beyond which BC becomes irrelevant), and $W(\bar{K}) = \bar{K}$ (the maximal possible value of the net worth), as well as the stability of the steady state.

In Region **A** of Fig. 3, $k_c \geq \bar{K}$ holds. In this case, the Bad never attract credit and all the credit goes to the Good, so that $k_{t+1} = W(k_t)$ for $k_t \in (0, \bar{K}]$. Then, from the monotonicity of W and A1, k_t converges monotonically to $k_L^* = \bar{K}$ for any $k_0 \in (0, \bar{K}]$, as shown in Fig. 4a. The condition, $k_c \geq \bar{K}$, can be rewritten as $f'(\bar{K}) \geq R(W(\bar{K})) = R(\bar{K})$ or

$$\mu B \leq f'(\bar{K}) \min\{1 - \bar{K}/m, \mu\} \tag{9}$$

This condition is met either when $B \leq f'(\bar{K})$ or when $\mu B \leq f'(\bar{K})(1 - \bar{K}/m)$. Thus, the Bad never attract credit, either when they are not very profitable (a small B) or have very low pledgeable return (a small μB).

[13] The two purposes of this extension are already discussed in footnote 2.

[14] No welfare connotations are intended by this choice of the terminology. Indeed, the financial frictions here create inefficiency by causing an over (under)-investment into the Good (Bad).

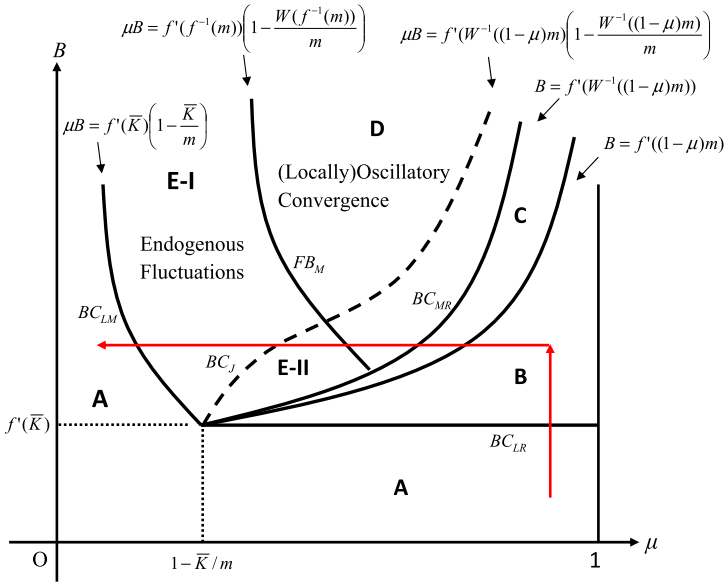

Fig. 3. **Parameter configuration**: $\bar{K} \equiv W(\bar{K}) < m < f(\bar{K})$. Assumption (A2), $\bar{K} < m$, ensures the existence of region **A** above the horizontal line, $B = f'(\bar{K})$. The parameter restriction, $m < f(\bar{K})$, ensures the existence of region **E**. The boundaries between **A** and **B** (BC_{LR}), between **B** and **C**, between **C** and **D/E-II** (BC_{MR}), between **E-I** and **E-II** (BC_J) and between **E-I** and **A** (BC_{LM}) are all issuing from the point, $(\mu, B) = (1 - \bar{K}/m, f'(\bar{K}))$. The boundaries between **B** and **C**, between **C** and **D** (BC_{MR}) and between **E-I** and **E-II** (BC_J) are all asymptotic to $\mu = 1$. The boundaries between **D** and **E** (FB_M) and between **E-I** and **A** (BC_{LM}) are hyperbolae and asymptotic to $\mu = 0$.

In the other four regions, $k_c < \bar{K}$, so the Bad attract credit and hence $k_{t+1} < W(k_t)$ for $k_t \in (k_c, \bar{K}]$. In Region **B** of Fig. 3, $k_\mu \le k_B = k_c < \bar{K}$ or

$$f'(\bar{K}) < B \le f'\big((1-\mu)m\big), \tag{10}$$

holds. As already discussed before, this condition ensures that BC is never binding whenever the Bad attract some credit, and hence $f'(k_{t+1}) = R(W(k_t)) = B$ for all $k_t \in (k_c, \bar{K}]$. The map is thus given by Eq. (8), which has two branches (upward in $\boldsymbol{L}$ and flat in $\boldsymbol{R}$), as shown in Fig. 1b. In addition, $k_B = k_c < \bar{K}$ ensures that the steady state is located on $\boldsymbol{R}$. The dynamics is hence monotone and mapped into the steady state, $k_R^* = w_B$ in finite time, as shown in Fig. 4b.

In Regions **C**, **D**, and **E**, $k_\mu > k_c > k_B$ holds. The map is thus given by Eq. (9), with three branches (upward $\boldsymbol{L}$, downward $\boldsymbol{M}$, and flat $\boldsymbol{R}$), as shown in Fig. 2b. In Region **C**, $k_c < k_\mu < w_B$ or

$$f'\big((1-\mu)m\big) < B < f'\big(W^{-1}\big((1-\mu)m\big)\big) \tag{11}$$

holds so that the map intersects with the 45° line in $\boldsymbol{R}$, the flat branch. Hence, BC is not binding in the steady state. In this case, the state is mapped into $k_R^* = w_B$ in finite time, as in **B**, but, unlike **B**, it is not globally monotone. For $k_0 < k_\mu < k_R^*$, the dynamics generally overshoots k_R^* and is mapped into it from above, as shown in Fig. 4c.

In Regions **D** and **E**, $k_c < k_\mu$ and $k_\mu > w_B$ hold so that the map intersects with the 45° line in $\boldsymbol{M}$. Thus, the Bad are active with the binding BC in a neighborhood of the steady state. By setting $k_t = k_{t+1} = k_M^*$ in $k_{t+1} = \Psi_M(k_t)$,

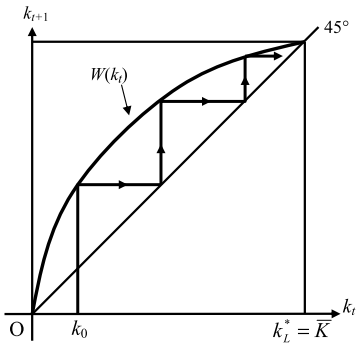

a) $(k_c \geq \overline{K})$ Global monotone converging to $k_L^* = \overline{K}$.

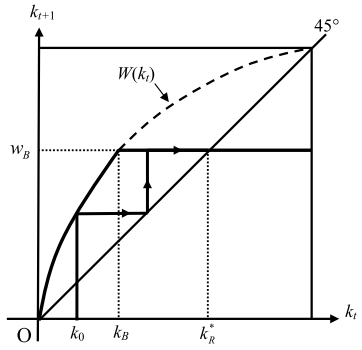

b) $(k_\mu \leq k_B = k_c < \overline{K})$
Globally mapped into $k_R^* = (f')^{-1}(B) = W(k_c)$.

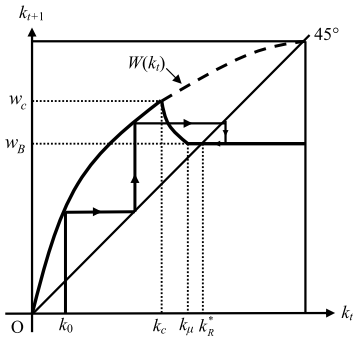

c) $(k_B < k_c < k_\mu \leq k_R^* = w_B)$:
Globally mapped into $k_R^* = w_B < w_c$ with over-shooting

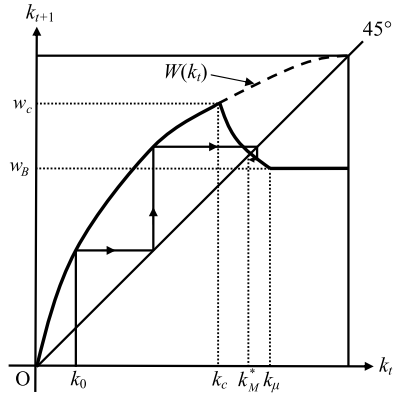

d) $(k_c < k_M^* < k_\mu)$ (Locally) oscillatory convergence to k_M^*.

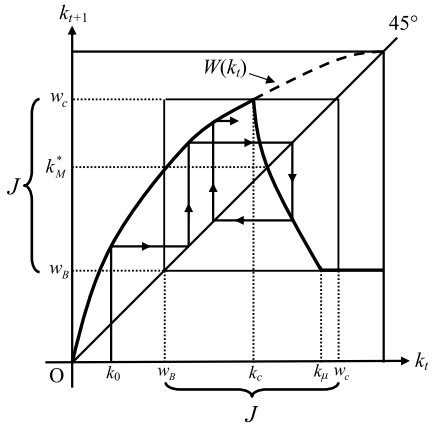

e) $(k_c < k_M^* < k_\mu)$ Endogenous fluctuations with the unstable steady state, k_M^*. Depending on whether the absorbing interval, *J,* includes the flat branch, there are two cases; **E-I,** where only two branches (*L* and *M*) are involved in *J*, and **E-II**, where all three branches (*L*, *M*, and *R*) are involved in *J*, as shown here.

Fig. 4. Phase diagrams.

$$\mu B = f'\big(k_M^*\big)\left(1 - \frac{W(k_M^*)}{m}\right). \tag{12}$$

The dynamics around k_M^* is oscillatory; it is locally stable in Fig. 4d and unstable in Fig. 4e. Differentiating $k_{t+1} = \Psi_M(k_t)$ and then setting $k_t = k_{t+1} = k_M^*$ yields

$$1 + \Psi'\big(k_M^*\big) = 1 - \frac{k_M^* f'(k_M^*)}{m - W(k_M^*)} = \frac{m - f(k_M^*)}{m - W(k_M^*)}.$$

Hence, the steady state k_M^* is locally asymptotically stable, $-1 < \Psi'(k_M^*) < 0$, if $f(k_M^*) < m$ and it is unstable, $\Psi'(k_M^*) < -1$, if $f(k_M^*) > m$. Since the right hand side of (12) is decreasing in k_M^*, the conditions for these two cases can be written as:

$$\mu B > f'\big(f^{-1}(m)\big)\left(1 - \frac{W(f^{-1}(m))}{m}\right) \quad \text{and} \quad B > f'\big(W^{-1}\big((1-\mu)m\big)\big), \tag{13}$$

and

$$f'(\bar{K})(1 - \bar{K}/m) < \mu B < f'\big(f^{-1}(m)\big)\left(1 - \frac{W(f^{-1}(m))}{m}\right) \quad \text{and}$$
$$B > f'\big(W^{-1}\big((1-\mu)m\big)\big), \tag{14}$$

as illustrated by **D** and **E** in Fig. 3. (The existence of Region **E** is ensured by $f(\bar{K}) > m$.)

In Region **E**, the equilibrium trajectory will eventually enter the interval, $J \equiv [\Psi(w_c), w_c]$ for any $k_0 \in (0, \bar{K}]$, and stay there forever. Furthermore, $\Psi(J) = J$. Hence, J is *invariant* and *absorbing*. If $W(k_c) = w_c < k_\mu$ – this is *not* the case depicted by Fig. 4e –, $w_B = \Psi(k_\mu) < \Psi(w_c) < w_c < k_\mu$ holds and hence $J \equiv [\Psi_M(w_c), w_c]$ overlaps with (upward) $\boldsymbol{L}$ and (downward) $\boldsymbol{M}$, but not with (flat) $\boldsymbol{R}$. This means that $\Psi(x) = k$ has at most two solutions for any $k \in J$, which means that the (unstable) steady state, k_M^*, has at most a countable number of pre-images. In other words, the equilibrium trajectory exhibits persistent fluctuation for almost all initial values, $k_0 \in (0, \bar{K}]$. Some algebra yields that this condition, $W(k_c) = w_c < k_\mu$, is given by

$$f'(\bar{K})(1 - \bar{K}/m) < \mu B < f'\big(f^{-1}(m)\big)\left(1 - \frac{W(f^{-1}(m))}{m}\right) \quad \text{and}$$
$$\mu B > f'\big(W^{-1}\big((1-\mu)m\big)\big)\left(1 - \frac{W^{-1}((1-\mu)m)}{m}\right), \tag{15}$$

shown as **E-I** in Fig. 3, the sub-region of Region **E** above the dashed curve. On the other hand, in **E-II** in Fig. 3, sub-region of Region **E** below the dashed curve,

$$f'(\bar{K})(1 - \bar{K}/m) < \mu B < f'\big(f^{-1}(m)\big)\left(1 - \frac{W(f^{-1}(m))}{m}\right) \quad \text{and}$$
$$\mu f'\big(W^{-1}\big((1-\mu)m\big)\big) < \mu B < f'\big(W^{-1}\big((1-\mu)m\big)\big)\left(1 - \frac{W^{-1}((1-\mu)m)}{m}\right), \tag{16}$$

$W(k_c) = w_c > k_\mu$ holds. In this case, $w_B = \Psi(k_\mu) = \Psi(w_c) < k_\mu < w_c$ and the absorbing interval, $J = [w_B, w_c]$, overlaps also with (flat) $\boldsymbol{R}$, as depicted in Fig. 4e. In this region, there exists a set of parameter values with measure zero, for which w_B is a pre-image of the (unstable) steady state, k_M^*, or of a point of an unstable cycle and the set of pre-images of w_B has a positive measure in $J = [w_B, w_c]$. Hence, for these parameter values, the equilibrium trajectory is mapped into the (unstable) steady state, k_M^*, or an unstable cycle in finite times for a positive measure of

initial values, $k_0 \in J$.[15] However, for almost all parameter values in **E-II**, w_B is not a pre-image of the (unstable) steady state, and hence the equilibrium trajectory exhibits persistent fluctuation for almost all initial values, $k_0 \in J$.

A First Look at Bifurcations:

Before proceeding, it would be instructive to see how the dynamical system changes its qualitative features, when the boundaries across these regions are crossed, as we move around the parameter space, (μ, B), for example, $\mathbf{A} \to \mathbf{B} \to \mathbf{C} \to \mathbf{D} \to \mathbf{E\text{-}II} \to \mathbf{E\text{-}I} \to \mathbf{A}$, as indicated by the red arrows in Fig. 3. This also gives us the opportunity to introduce various types of *bifurcations* informally to prepare the reader for a more detailed bifurcation analysis to come.

Let us start in Region **A** with $B < f'(\bar{K})$ and with μ very close to 1. Then, the upward $\boldsymbol{L}$ branch covers the entire range, $(0, \bar{K}]$, and the steady state is given by $k_L^* = \bar{K}$, as shown in Fig. 4a. As we increase B, the flat $\boldsymbol{R}$ branch shifts down and moves left, causing the $\boldsymbol{L}$ branch to shrink. This causes the flat $\boldsymbol{R}$ branch to collide with $k_L^* = \bar{K}$, at which point the steady state undergoes a *border collision bifurcation* (BCB), BC_{LR}, at the boundary between Regions **A** and **B**, where $k_L^* = \bar{K} = k_R^*$, which is given by:

$$BC_{LR}: \quad B = f'(\bar{K}).$$

Once we enter **B**, the steady state is now given by $k_R^* = w_B > k_B > k_\mu$, as shown in Fig. 4b. Now, as we decrease μ and cross the boundary between Regions **B** and **C**, given by $B = f'((1-\mu)m) > f'(\bar{K})$, we enter Region **C**, $k_B < k_c < k_\mu < w_B = k_R^*$, where the downward $\boldsymbol{M}$ branch emerges, as shown in Fig. 4c. A further decrease in μ causes the downward $\boldsymbol{M}$ branch to shift right and collide with $k_R^* = w_B$, where the steady state undergoes a BCB, BC_{MR}, at the boundary of Regions **C** and **D**, where $k_M^* = k_\mu = k_R^*$, which is given by:

$$BC_{MR}: \quad B = f'\big(W^{-1}\big((1-\mu)m\big)\big) > f'\big((1-\mu)m\big).$$

Once we enter **D**, the steady state is now k_M^*, and, with $\Psi'(k_M^*) > -1$, it is asymptotically stable as shown in Fig. 4d. Then, as we reduce μ further, the downward $\boldsymbol{M}$ branch continues to shift right and becomes steeper, causing k_M^* to lose its stability via a *flip bifurcation*, FB_M, at the boundary between Regions **D** and **E**, where $\Psi'(k_M^*) = -1$, which is given by:

$$FB_M: \quad \mu B = f'\big(f^{-1}(m)\big)\left(1 - \frac{W(f^{-1}(m))}{m}\right) \quad \text{for } B > f'\big(W^{-1}\big((1-\mu)m\big)\big),$$

after which the steady state k_M^* is unstable with $\Psi'(k_M^*) < -1$. As we enter **E** below the dashed curve separating **E-I** and **E-II**, we are in **E-II**, as shown in Fig. 4e, where the absorbing interval, J, covers all three branches. With a further decrease in μ, k_μ collides with w_c, hence the absorbing interval, J, at

$$BC_J: \quad \mu B = f'\big(W^{-1}\big((1-\mu)m\big)\big)\left(1 - \frac{W^{-1}((1-\mu)m)}{m}\right),$$

and we enter Region **E-I**, where the absorbing interval, J, covers only two branches, $\boldsymbol{L}$ and $\boldsymbol{M}$. Finally, as we decrease in μ further, the downward $\boldsymbol{M}$ branch continues to shift right, causing k_M^* to collide with $\bar{K}$ and the system undergoes another BCB, BC_{LM}, at the boundary of Region **A** and **E-I**, where $k_M^* = \bar{K} = k_L^*$, which is given by:

[15] An unstable invariant set that attracts a positive measure of the initial conditions is called a *Milnor attractor*.

$$BC_{LM}: \quad \mu B = f'(\bar{K})(1 - \bar{K}/m),$$

after which we find ourselves again in Region **A**, as shown in Fig. 4a.[16]

Of particular interest among all the regions shown in Fig. 3 are regions **D** and **E**, i.e., when the Bad are sufficiently profitable, $B > f'(\bar{K})$ and their pledgeability, μ, is neither too high nor too low. In these regions, the pledgeability problem is significant enough (i.e., μ is not too high) that the credit continues to flow into the Good, even if its rate of return is strictly less than B. Of course, the agents are eager to take advantage of the low equilibrium rate of return by running the Bad projects, but some of them are unable to do so due to BC. If μ is not too low, an improvement in net worth would ease BC, which drives up the equilibrium rate of return. This in turn causes a decline in the investment into the Good, which reduces the net worth of the agent in the next period. When μ is relatively high (i.e., in region **D**), this effect is not strong enough to make the steady state unstable. When μ is relatively low (i.e., in region **E**), this effect is strong enough to make the steady state unstable and generate endogenous fluctuations. Thus, the following proposition may be stated.

Proposition 1 *(Effects of μ). For any $B > f'(\bar{K})$, endogenous fluctuations occur (almost surely) for an intermediate range of μ.*

Endogenous credit fluctuations thus occur when the Bad are sufficiently profitable and when their pledgeability problem is large enough that the agents cannot finance it when their net worth is low, but small enough that they can finance it when their net worth is high.

Region **D** is also of some interest, because the local convergence toward the steady state is oscillatory. If the economy is hit by recurrent shocks, the equilibrium dynamics exhibit considerable fluctuations even in a neighborhood of the steady state.[17] A quick look at Fig. 3 verifies that a sufficiently high B ensures that the economy is in Region **D**. Thus, another proposition may be stated.

Proposition 2 *(Effects of B). For any $\mu \in (0, 1)$, the dynamics around the steady state is oscillatory for a sufficiently high B.*

The intuition behind this result is easy to grasp. When the agents are sufficiently eager to run the Bad projects (because they are sufficiently profitable), their borrowing constraint becomes binding in the presence of financial frictions. A higher net worth in the current period eases the borrowing constraint, which drives up the equilibrium rate of return, which reduces the credit flow to the Good, which leads to a lower net worth in the next period.

As already pointed out, persistent fluctuations occur for almost all initial conditions everywhere in **E-I**, while this is true only for almost all parameter values in **E-II**. However, this is not the only significant difference between the two regions. It turns out that the types of fluctuations

[16] If we reduce μ at a value of B higher than indicated by the red arrow, the system can skip **E-II** and move directly from **D** to **E-I** via a flip bifurcation, as it crosses FB_M. If we reduce μ at a value of B lower than indicated by the red arrow, the system can skip **D** and move directly from **C** to **E-II** via a *border-flip bifurcation*, as it crosses BC_{MR}, where $w_B = k_M^* = k_\mu = k_R^*$ and $\Psi'(k_M^*) < -1$.

[17] In addition, endogenous fluctuations may occur in region **D**, because the local stability of the unique steady state does not guarantee the global stability. Indeed, as seen in Section 4.2, a stable period-2 cycle can coexist with the stable steady state near the boundary of **D** and **E** on the side of region **D**.

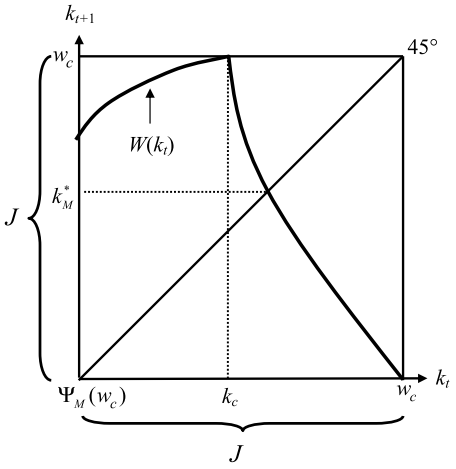

Fig. 5a. Map restricted on the absorbing interval, J, above BC_J.

observed in **E-I** and **E-II** are totally different in nature. Those observed in **E-II** display certain peculiar features due to the presence of the flat branch in the absorbing interval. Though these features are mathematically quite intriguing, their economic significances are not obvious.[18] For this reason, we focus on **E-I** in this paper, leaving a detailed analysis of **E-II** in our companion paper, Sushko et al. (2014a).

With our focus on **E-I**, where the absorbing interval overlaps only with $\boldsymbol{L}$ and $\boldsymbol{M}$, we may rewrite Eq. (6), by restricting it to $J \equiv [\Psi_M(w_c), w_c]$, as follows:

$$k_{t+1} = \Psi_J(k_t) = \begin{cases} \Psi_L(k_t) \equiv W(k_t) & \text{if } \Psi_M(w_c) \le k_t < k_c \\ \Psi_M(k_t) \equiv (f')^{-1}\left(\frac{\mu B}{1-W(k_t)/m}\right) & \text{if } k_c \le k_t \le w_c, \end{cases} \tag{17}$$

which has one kink, separating the upward $\boldsymbol{L}$ branch and the downward $\boldsymbol{M}$ branch, as shown in Fig. 5a. Notice that the parameters, μ and B, enter in Eq. (17) only through its product, μB, the pledgeable rate of return. Hence, if we restrict our attention to this region, we can classify the dynamical system into three cases in the parameter space, $(m, \mu B)$ as follows.

Proposition 3 *(Effects of μB). For a sufficiently large B, our map, Eq. (6), when restricted to its absorbing interval, $J \equiv [\Psi_M(w_c), w_c]$, is reduced to Eq. (17), which depends solely on m, μB and $f(\bullet)$. Furthermore, for $m < f(\bar{K})$,*

i) *For $\mu B < f'(\bar{K})(1 - \frac{\bar{K}}{m})$, the map is in Region* **A**, *where the Bad never attract credit and all the credit goes to the Good, and k_t monotonically converges to $k_L^* = \bar{K}$.*

ii) *For $f'(\bar{K})(1 - \frac{\bar{K}}{m}) < \mu B < f'(f^{-1}(m))(1 - \frac{W(f^{-1}(m))}{m})$, the map is in Region* ***E-I****, where the equilibrium path persistently fluctuates around k_M^* for almost all initial conditions.*

iii) *For $\mu B > f'(f^{-1}(m))(1 - \frac{W(f^{-1}(m))}{m})$, the map is in Region* **D**, *where the equilibrium path oscillates and converges towards k_M^* locally.*

[18] For example, if a Bad project generates $m\varepsilon > 0$ units of physical capital in addition to mB units of the final good, the right branch becomes increasing, no matter how small $\varepsilon > 0$ is.

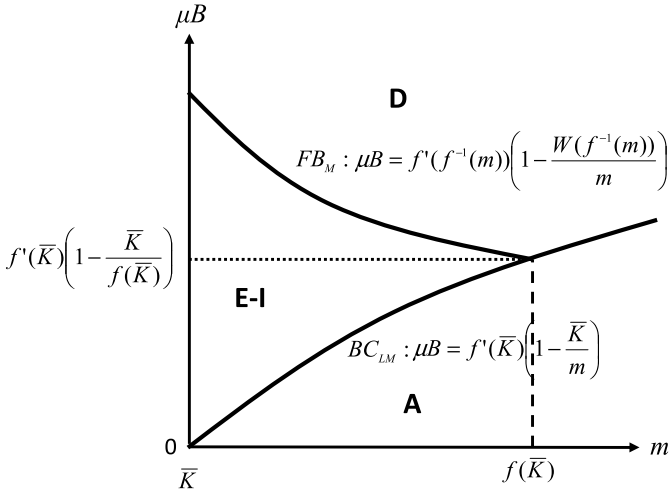

Fig. 5b. Parameter configuration in $(m, \mu B)$ above BC_J.

Fig. 5b illustrates Proposition 3, where **E-I** is now bounded by **A** from below and **D** from above, and its existence requires $m < f(\bar{K})$. This shows that the unique steady state is unstable and endogenous fluctuations arise for an intermediate range of μB, that is, when the pledgeable rate of return of the Bad projects is neither too low nor too high. Note that the unique steady state loses its stability in different ways at the two ends of the instability range of μB. At the upper end (on the FB_M curve), a decline in μB leads to the instability of the steady state via a *flip bifurcation*. At the lower end (on the BC_{LM} curve), an increase in μB leads to the instability of the steady state via a *BCB*. Hence, the nature of fluctuations observed at these ends can be very different, as will be explained in the next section.

4. Dynamics analysis: Cobb–Douglas case

To make further progress and to understand the nature of fluctuations, we now turn to a special case where the production function is Cobb–Douglas: $f(k) = A(k)^\alpha$ with $\alpha \in (0, 1)$, so that $w_t = W(k_t) = (1-\alpha)A(k_t)^\alpha$. It turns out that it is more convenient to write the dynamics in w_t, instead of k_t. After the normalization, $(1-\alpha)A = 1$, $w_t = W(k_t) = (k_t)^\alpha$ and thus Eq. (6) can be written as:

$$w_{t+1} = T(w_t) \equiv \begin{cases} T_L(w_t) \equiv (w_t)^\alpha & \text{if } w_t \le w_c \\ T_M(w_t) \equiv [\frac{1}{\mu B}(\frac{\alpha}{1-\alpha})(1-\frac{w_t}{m})]^{\frac{\alpha}{1-\alpha}} & \text{if } w_c \le w_t \le w_\mu \\ T_R(w_t) \equiv (\frac{\alpha}{B(1-\alpha)})^{\frac{\alpha}{1-\alpha}} \equiv w_B & \text{if } w_t \ge \max\{w_c, w_\mu\}, \end{cases} \tag{18}$$

where w_c is given by $(w_c)^{1-\alpha} \equiv \frac{\alpha}{\mu B(1-\alpha)} Max\{1-\frac{w_c}{m}, \mu\}$, satisfying $T_L(w_c) \equiv T_M(w_c)$ and $w_\mu \equiv m(1-\mu)$, so that $T_M(w_\mu) \equiv T_R(w_\mu)$. Eq. (18) is thus a continuous piecewise smooth dynamical system, with four parameters, α, μ, m, B, with the restrictions, $0 < \alpha, \mu < 1$, $B > 0$, and $(1-\alpha)m < 1 < m$. With the normalization, $(1-\alpha)A = 1$, $W(\bar{K}) = \bar{K} = 1$, and hence T maps $(0, 1]$ into itself. From now on, we restrict T on $(0, 1]$.

4.1. Some preliminaries

As done in Fig. 3, the parameter space (μ, B) can be divided into regions, **A**, **B**, **C**, **D**, **E-I**, and **E-II**, for a given (α, m). In Region **A**, the dynamics converge to the unique steady state in L, $w_L^* = 1$. Its boundary with **B** is the BCB curve,

$$BC_{LR}: \quad B = \frac{\alpha}{1-\alpha} \quad \text{for } \mu \geq 1 - \frac{1}{m}$$

on which $w_L^* = 1 = w_R^*$ holds. Its boundary with **E-I** is the BCB curve,

$$BC_{LM}: \quad \mu B = BC_{LM}(\alpha, m) \equiv \left(\frac{\alpha}{1-\alpha}\right)\left(1 - \frac{1}{m}\right) \quad \text{for } \mu \leq 1 - \frac{1}{m}$$

on which $w_L^* = 1 = w_c = w_M^*$ holds. In Regions **B** and **C**, the dynamics converge to the unique steady state, w_R^*, located in R. The outer boundary of **C** (with **D** and **E**) is the BCB curve,

$$BC_{MR}: \quad B = \left(\frac{\alpha}{1-\alpha}\right)\left[m(1-\mu)\right]^{1-1/\alpha} \quad \text{for } \mu \geq 1 - \frac{1}{m}$$

on which $w_M^* = w_\mu = w_R^*$ holds. In Region **D**, the unique steady state, w_M^*, located in M, is locally stable, because $0 > T'(w_M^*) > -1$. In Region **E**, it is locally unstable, because $T'(w_M^*) < -1$. As we move from **D** to **E**, w_M^* loses its stability via a flip bifurcation, $T'(w_M^*) = -1$. Thus, the boundary between **D** and **E** is given by the flip bifurcation curve,

$$FB_M: \quad \mu B = FB_M(\alpha, m) \equiv \left(\frac{\alpha^2}{1-\alpha}\right)\left[(1-\alpha)m\right]^{1-1/\alpha}$$
$$\text{for } B > \left(\frac{\alpha}{1-\alpha}\right)\left[m(1-\mu)\right]^{1-1/\alpha}.$$

In Region **E**, bounded by BC_{LM} (from the left), FB_M (from the right) and BC_{MR} (from below), the unique steady state, w_M^*, is unstable, and there exists an absorbing interval, J, whose upper bound is given by $T(w_c)$. In Region **E-I**, $T(w_c) \leq w_\mu$ holds so that only the upward ***L***-branch and the downward ***M***-branch are involved when T is restricted on $J = [T^2(w_c), T(w_c)]$, so that:

$$w_{t+1} = T_J(w_t) \equiv \begin{cases} T_L(w_t) \equiv (w_t)^\alpha & \text{for } T^2(w_c) \leq w_t \leq w_c \\ T_M(w_t) \equiv \left[\frac{\alpha}{\mu B(1-\alpha)}\left(1 - \frac{w_t}{m}\right)\right]^{\frac{\alpha}{1-\alpha}} & \text{for } w_c \leq w_t \leq T(w_c). \end{cases} \tag{19}$$

In Region **E-II**, $T(w_c) > w_\mu$ holds so that all three branches, including the flat ***R***-branch is involved and $J = [w_B, T(w_c)]$. The boundary between **E-I** and **E-II** is given by $T(w_c) = w_\mu$, i.e.,

$$BC_J: \quad \mu B = \left(\frac{\alpha}{1-\alpha}\right)\left(\mu - 1 + \left[m(1-\mu)\right]^{1-1/\alpha}\right)$$

between BC_{LM} and FB_M.

As already mentioned, the types of fluctuations observed in **E-I** and **E-II** are totally different. In what follows, we will report some results from Sushko et al. (2014b; henceforth SGM), which conducts a detailed bifurcation analysis on **E-I**, particularly on the nature of transition as we move from **D** to **E-I** by crossing the FB_M curve or from **A** to **E-I** by crossing the BC_{LM} curve. For the analysis of **E-II**, as well as the transition between **E-I** and **E-II**, we refer to another companion paper of ours, Sushko et al. (2014a).

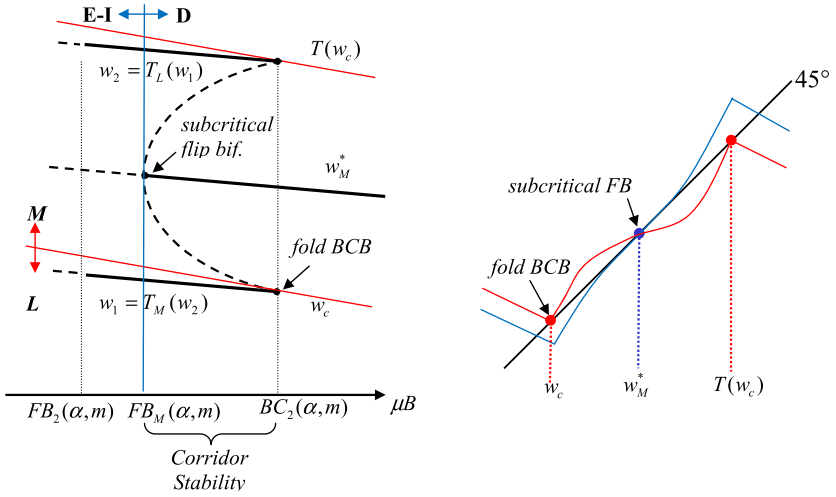

Fig. 6. Crossing the FB_M curve for $\alpha < 0.5$: subcritical FB and fold BCB. (For interpretation of the references to color in this figure, the reader is referred to the web version of this article.)

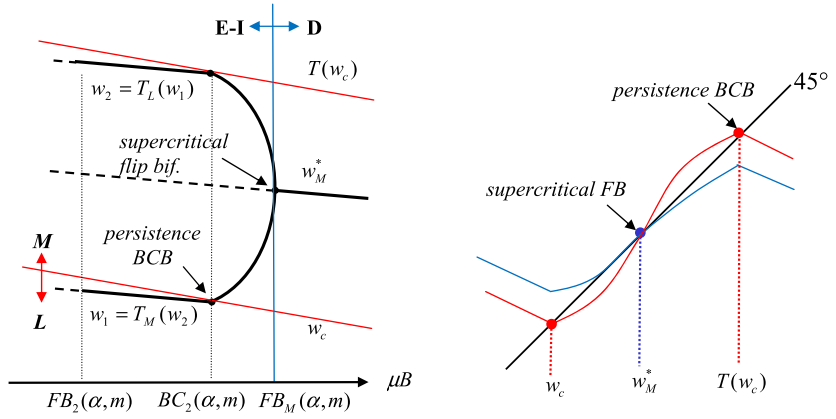

Fig. 7. Crossing the FB_M curve for $\alpha > 0.5$: supercritical FB and persistence BCB. (For interpretation of the references to color in this figure, the reader is referred to the web version of this article.)

4.2. *Crossing the FB_M curve: corridor stability*[19]

Let us first describe what happens when we move from **D** to **E-I** and cross the FB_M curve by decreasing μB. The left panels of Fig. 6 and Fig. 7 show the graphs of w_M^*, w_c, $T(w_c)$, as well as period-2 cycles, as functions of μB. Also shown are the three critical values of μB:

- $FB_M(\alpha, m)$, at which $T'(w_M^*) = -1$ (the flip bifurcation of w_M^* occurring at the boundary between **D** and **E-I**);
- $BC_2(\alpha, m)$, at which $T^2(w_c) = w_c$ (the existence of the period-2 cycle, $w_c \leftrightarrow T(w_c)$);

[19] Much of this section is based on Section 4 of SGM.

- $FB_2(\alpha, m)$, at which $(T_M \circ T_L)'(w_1) = -1$, where w_1 is given by $(T_M \circ T_L)(w_1) = w_1$ (the flip bifurcation of the period-2 cycle that alternates between the $\boldsymbol{L}$- and the $\boldsymbol{M}$-branch, $w_1 = T_M(w_2) \leftrightarrow T_L(w_1) = w_2$).[20]

Fig. 6 illustrates the case of $\alpha < 0.5$, for which $BC_2(\alpha, m) > FB_M(\alpha, m) > FB_2(\alpha, m)$ holds. For $\mu B > BC_2(\alpha, m)$, the unique steady state, w_M^*, is not only stable (as indicated by the solid line) but also globally attracting. At $\mu B = BC_2(\alpha, m)$, the period-2 cycle, $w_c \leftrightarrow T(w_c)$, is born via *a fold BCB*. On the right panel, this is depicted by the graph of $T^2(w)$ in Red, which touches the 45° line at $w = w_c$ and $w = T(w_c)$. As μB declines further, this period-2 cycle is split into a pair of period-2 cycles, one stable (as indicated by the pair of the solid lines on the left panel), $w_1 = T_M(w_2) \leftrightarrow T_L(w_1) = w_2$, alternating between $\boldsymbol{L}$ and $\boldsymbol{M}$, and one unstable (as indicated by the dashed curves on the left panel), oscillating within the $\boldsymbol{M}$-branch.[21] For $FB_M(\alpha, m) < \mu B < BC_2(\alpha, m)$, the stable steady state, w_M^*, co-exists with the stable period-2 cycle. Their basins of attraction are separated by the unstable period-2 cycle and its pre-images. Then, as μB continues to decrease and moves toward the boundary with **E-I**, the unstable period-2 cycle approaches and merges with the steady state, w_M^*, and disappears at the *subcritical* flip at $\mu B = FB_M(\alpha, m)$. On the right panel, this is depicted by the graph of T^2 in Blue, which is concave in (w_c, w_M^*) and convex in $(w_M^*, T(w_c))$ for $\alpha < 0.5$ with w_M^*, the inflection point, being tangent to the 45° line.[22] Upon entering **E-I**, the steady state w_M^* becomes unstable (as indicated by the dashed line), while the period-2 cycle alternating between $\boldsymbol{M}$ and $\boldsymbol{L}$, $w_1 = T_M(w_2) \leftrightarrow T_L(w_1) = w_2$, remains stable. This continues, as long as $FB_M(\alpha, m) > \mu B > FB_2(\alpha, m)$, i.e., until this period-2 cycle loses its stability via a flip bifurcation at $\mu B = FB_2(\alpha, m)$.[23]

Fig. 7 illustrates the case of $\alpha > 0.5$, for which $FB_M(\alpha, m) > BC_2(\alpha, m)$ holds. Fig. 7 further assumes $BC_2(\alpha, m) > FB_2(\alpha, m)$, which holds for α not too large. As shown on the left panel, the unique steady state, w_M^*, is globally attracting in **D**, i.e., for $\mu B > FB_M(\alpha, m)$. Then, it undergoes a *supercritical* flip at the boundary with **E-I**, i.e., at $\mu B = FB_M(\alpha, m)$. On the right panel, this is depicted by the graph of T^2 in Blue, which is convex in (w_c, w_M^*) and concave in $(w_M^*, T(w_c))$ for $\alpha > 0.5$ with w_M^*, the inflection point, being tangent to the 45° line. As $\mu B < FB_M(\alpha, m)$, the steady state becomes unstable, which creates a stable period-2 cycle. This cycle oscillates

[20] Some algebra yields $FB_2(\alpha, m) = (\alpha\gamma^2/(1+\alpha\gamma))((1+\alpha\gamma)/m)^{1/\alpha\gamma}$, where $\gamma = \alpha/(1-\alpha)$. Generally, $BC_2(\alpha, m)$ can be defined only implicitly.

[21] As shown on the right panel, $T^2(w) = T_M \circ T_L(w)$ is decreasing in $w < w_c$ and $T^2(w) = T_M^2(w)$ is increasing in $w > w_c$; $T^2(w)$ has thus a kink at $w = w_c$. Before this BCB, $T^2(w_c) > w_c$ and, for $\alpha < 0.5$, T^2 intersects with the 45° line only at w_M^*, so there is no period-2 cycle, hence no cycle of any periodicity. At the BCB, where $T^2(w_c) = w_c$, the left derivative of T^2 at w_c satisfies $0 > (T_M \circ T_L)'(w_c) > -1$ and the right derivative satisfies $(T_M^2)'(w_c) > 1$. After this BCB, $T^2(w_c) < w_c$ holds, thereby creating two intersections with the 45° line, one below w_c and one above w_c. The period-2 cycle alternating between L and M is stable because it corresponds to the first intersection where the slope of T^2 is less than one in absolute value. The period-2 cycle confined with M is unstable, because it corresponds to the second intersection where the slope of T^2 is greater than one.

[22] Note that, when w_M^*, as the fixed point of T, undergoes a flip bifurcation $T'(w_M^*) = -1$ to create a period-2 cycle of T, w_M^*, as the fixed point of T^2, undergoes a pitchfork bifurcation, $(T^2)'(w_M^*) = 1$, to create a new pair of the fixed points of T^2, neither of which is a fixed point of T.

[23] This last statement, and the left panel of Fig. 6, assume $m < 1 + \alpha^2/(1-\alpha)$ so that $\mu B = FB_2(\alpha, m) > BC_{LM}(\alpha, m)$, which is necessary for the flip bifurcation of this period-2 cycle to occur in **E-I**. If $m > 1 + \alpha^2/(1-\alpha)$, $FB_2(\alpha, m) < BC_{LM}(\alpha, m)$, and hence this period 2-cycle never undergoes a flip bifurcation, as μB declines. Instead, it shrinks and converges to $w_L^* = 1$ and disappears at the BC_{LM} curve. Indeed, we will show later that the period-2 occurs immediately after crossing the BC_{LM} curve from **A** to **E-I** under the condition, $m > 1 + \alpha^2/(1-\alpha)$. See also Fig. 10.

entirely within the M-branch for $FB_M(\alpha, m) > \mu B > BC_2(\alpha, m)$. Then, at $\mu B = BC_2(\alpha, m)$, this cycle collides with the border with w_c. On the right panel, this is depicted by the graph of $T^2(w)$ in Red, with $T^2(w_c) = w_c$. When α is not too large and hence $BC_2(\alpha, m) > FB_2(\alpha, m)$ holds, one can show that the left derivative of T^2 at $w = w_c$ is less than one in absolute value. This ensures that, after the BCB, when T^2 intersects with the 45° line below $w = w_c$, its slope is less than one in absolute value for $BC_2(\alpha, m) > \mu B > FB_2(\alpha, m)$, so that the period-2 cycle alternating between $\boldsymbol{M}$ and $\boldsymbol{L}$, $w_1 = T_M(w_2) \leftrightarrow T_L(w_1) = w_2$, is stable.[24] This cycle then loses its stability at $\mu B = FB_2(\alpha, m)$.[25]

What happens for the non-generic case of $\alpha = 0.5$? In this case, the map is linear in the M-branch. The unique steady state, w_M^*, is stable and globally attracting, until $\mu B = FB_M(1/2, m) = BC_2(1/2, m) = 1/m$, where w_M^* loses its stability via a *degenerate* flip, which creates a continuum of (not asymptotically) stable period-2 cycles, with any point in $[w_c, w_M^*) \cup (w_M^*, T(w_c)]$ being 2-periodic. For $FB_M(1/2, m) = BC_2(1/2, m) > \mu B > FB_2(1/2, m)$, there exists a stable period-2 cycle, alternating between $\boldsymbol{M}$ and $\boldsymbol{L}$. This becomes unstable at $\mu B = FB_2(1/2, m) = 3/(4m^2)$.

Of particular interest is the empirically relevant case of $\alpha < 0.5$, illustrated in Fig. 6. For $BC_2(\alpha, m) > \mu B > FB_M(\alpha, m)$, i.e., between the subcritical flip of the steady state and the fold BCB, the locally stable steady state co-exists with the locally stable period-2 cycle. And the basin of attraction of the steady state is bounded by the unstable period-2 points, suggesting that the steady state possesses the corridor stability *a la* Leijonhufvud (1973): i.e., it is stable and self-correcting against small shocks but unstable against large shocks. Furthermore, when a parameter change causes the steady state to lose its stability via the subcritical flip, its effects are both *catastrophic* and *irreversible*. They are catastrophic in the sense that, when the economy, initially located in the steady state, becomes dislocated due to the parameter change, it converges to the period-2 cycle that is far away from the steady state, causing it to fluctuate widely, no matter how small the parameter change is. In other words, the effects are discontinuous in the parameter change. Furthermore, these effects are irreversible in the sense that reversing the parameter to the original value and restoring the stability of the steady state do not allow the economy to return to the steady state, because the period-2 cycle remains stable.[26] This suggests, among other things, that even a small, temporary credit crunch shock, captured by a small, one-time reduction in μ, could have large, permanent effects on the volatility.

Why do smaller values of α ensure the corridor stability? In other words, how does the unique steady state manage to maintain its local stability at least for a while when a decline in μB causes global instability of the dynamical system? The intuition is quite simple. In a neighborhood of the steady state, w_M^*, both the Good and the Bad projects are financed so that $R(w_t) = r_{t+1} = f'(k_{t+1})$ holds. As a small increase in the net worth w_t would allow the agents running the Bad projects to offer a higher rate of return to the lender, this bids up the equilibrium rate of return, r_{t+1}, which causes a decline in the capital-labor ratio, k_{t+1}. However, with a small share of

[24] For α sufficiently close to one, $BC_2(\alpha, m) < FB_2(\alpha, m)$. In this case, at the BCB, where $T^2(w_c) = w_c$, the left derivative of T^2 at $w = w_c$ is greater than one in absolute value. This implies that, immediately after the BCB, the period-2 cycle alternating between $\boldsymbol{M}$ and $\boldsymbol{L}$ is unstable and the dynamics converges to a chaotic attractor.

[25] Again, this last statement, and the left panel of Fig. 7, assume $m < 1 + \alpha^2/(1-\alpha)$ so that $\mu B = FB_2(\alpha, m) > BC_{LM}(\alpha, m)$. See also footnote 22.

[26] For the supercritical case of $\alpha > 0.5$ (shown in Fig. 7), the size of fluctuations along the stable period-2 cycle created by the flip increases continuously with the parameter. Thus, if the parameter change is reversed, the stable cycle shrinks and merges to the steady state, which allows the economy to return to it.

capital in the final goods production, a small decline in k_{t+1} is enough to restore the equilibrium, which means that the negative effect on $w_{t+1} = W(k_{t+1})$ is small, which dampens the effect of a small increase in w_t.

4.3. Crossing the BC_{LM} curve[27]

Let us now describe what happens immediately after an increase in μB leads to a transversal crossing of the BC_{LM} curve from **A** to **E-I**, which causes $w_L^* = 1$ to disappear. This can be done by using the following piecewise linear map:

$$x_{t+1} = \tau(x_t) = \begin{cases} \tau_L(x_t) = ax_t + 1 & \text{if } x_t < 0 \\ \tau_R(x_t) = bx_t + 1 & \text{if } x_t \geq 0, \end{cases} \tag{20}$$

with

$$\begin{aligned} a &= \lim_{w \uparrow 1} T'(w) = \alpha \in (0, 1), \\ b &= \lim_{w \downarrow 1} T'(w) = -\frac{\alpha}{(1-\alpha)(m-1)} \equiv B_m(\alpha) \in (-\infty, -1), \end{aligned} \tag{21}$$

as an approximation of our map.[28] Fig. 8a shows the graph of (20), while Fig. 8b shows the graph of the map, (17), to be approximated. The piecewise linear map, (20), is called *the skew tent map*, which has been fully characterized. See Sushko et al. (2015) for the detail. This map has quite rich dynamics. An attracting cycle of any period, as well as a robust chaotic attractor with any number of intervals, exists for an open region of the parameter space, (a, b), some of which can be seen in the bifurcation diagram in the (a, b) plane, shown in Fig. 9a (with Fig. 9b showing an enlargement of its boxed area). In Fig. 9a, the colored area with the number, 2, 3, 4, or 5, is the parameter region for the stable cycle with the number indicating its periodicity.[29] It can be shown that the stable n-cycle visits the downward-sloping branch only every n-th period, such that $x_1 = \tau(x_0) < x_2 < \ldots < x_{n-1} < 0 < x_0$.[30] In both Figs. 9a and 9b, the yellow area, marked as Q_1, represents the parameter region for a chaotic attractor with one interval. Various white regions in Fig. 9b, marked as $Q_{n,2n}$ or $Q_{n,n}$ $(n \geq 2)$, are the regions of a chaotic attractor with multiple intervals (with the second subscript indicating the number of intervals). On a chaotic attractor with n intervals, a trajectory visits each interval every $n-$th period, but when it returns to the same interval, it never repeats the same value, so that the trajectory ends up filling each interval. Thus, to the naked eye, the trajectory looks like an n-cycle with random noises.[31]

Using (21), the bifurcation diagram of the skew tent map can be mapped into the bifurcation diagram in the (α, m) plane, as shown in Fig. 10. For example, the region of the stable period-2 cycle for the skew tent map, $\{(a, b)| -1 < ab < -a\}$, shown in green, is mapped into $\{(\alpha, m)|1 -$

[27] Much of this section is based on Section 3 of SGM.

[28] In the language of the dynamical system theory, we use Eq. (20) as a *normal form* for a border collision bifurcation: see Sushko et al. (2015). Intuitively, as we approach BC_{LM} from the interior of **E-I**, $w_c \to 1$, $T(w_c) \to 1$ and $T^2(w_c) \to 1$, hence, the absorbing interval, $J = [T^2(w_c), T(w_c)]$, is sufficiently small near the BC_{LM} curve, which allows us to linearize our map around w_c.

[29] From the Li–Yorke theorem, we know that there exist an n-cycle for any $n \geq 2$ as well as a chaotic trajectory in the parameter region of the stable 3-cycle. However, the stable-3 cycle is a unique attractor in its region, to which the equilibrium trajectory converges from almost all initial conditions.

[30] The upper boundary of the region of the stable n-cycle is given by $b = -\frac{1-a^{n-1}}{(1-a)a^{n-2}}$. For $n \geq 3$, the stable n-cycle collides with the unstable n-cycle, also existing in the stable region, and disappears via a *fold BCB* at the upper boundary.

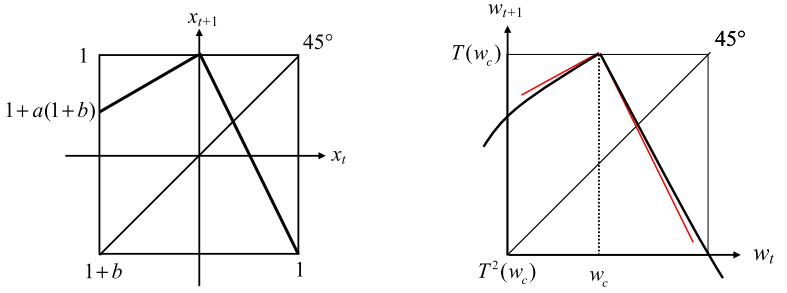

a) Skew Tent Map ($0<a<1; b<-1$) b) Eq. (19) after crossing the BC_{LM} curve

Fig. 8. Skew tent map as a border collision normal form.

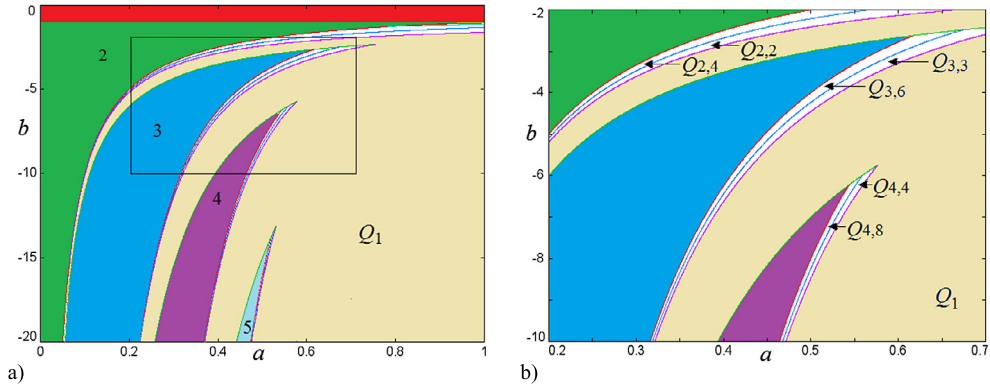

Fig. 9. Bifurcation diagrams for skew tent map. In Fig. 9a, the numbers, 2, 3, 4, and 5, in the colored regions indicate the periodicity of stable cycles. The yellow region, Q_1, indicates the region of a chaotic attractor with one interval. A magnification of the boxed area in Fig. 9a is shown in Fig. 9b. The white regions indicate the regions of a chaotic attractor with multiple intervals, with the second subscript indicates the number of intervals. See Sushko et al. (2015) for more detail. (For interpretation of the references to color in this figure legend, the reader is referred to the web version of this article.)

$\alpha+\alpha^2<(1-\alpha)m<1\}$, also shown in green.[32] And the region of $Q_{n,2n}$ is mapped into the region of $G_{n,2n}$, etc. From Fig. 10, we can thus find out what happens after the disappearance of the steady state, $w_L^*=1$, for generic values of (α, m). Note that, for any $a\in(0,1)$ and $b\in(-\infty,-1)$, the inverse of (21), $\alpha=a$ and $m=1-a/[(1-a)b]$, satisfies the model's parameter

The lower boundary of the region of the stable n-cycle is given by $b=-a^{1-n}$. The stable n-cycle loses its stability via a *degenerate flip bifurcation* at this boundary.

[31] The first subscript indicates how these chaotic attractors with multiple intervals are born. Starting from the region of the stable n-cycle, a reduction in b causes the n-cycle to lose its stability via a *degenerate flip bifurcation*, leading to a chaotic attractor with $2n$ intervals in $Q_{n,2n}$. A further reduction in b causes a pairwise merging of these intervals via a *merging bifurcation*, leading to a chaotic attractor with n intervals in $Q_{n,n}$. And a further reduction in b causes a sudden expansion of the size of these intervals, via an *expansion bifurcation*, leading to a chaotic attractor with one interval in Q_1.

[32] Notice that one of these conditions for the stable period-2 cycle holds automatically due to the model's parameter restriction, $(1-\alpha)m<1$. The other condition can be rewritten as $m>1+\alpha^2/(1-\alpha)$, so that $FB_2(\alpha,m)<BC_{LM}(\alpha,m)$, ruling out the possibility of the flip bifurcation of the period-2 cycle born at the FB_M curve. See footnotes 22 and 24.

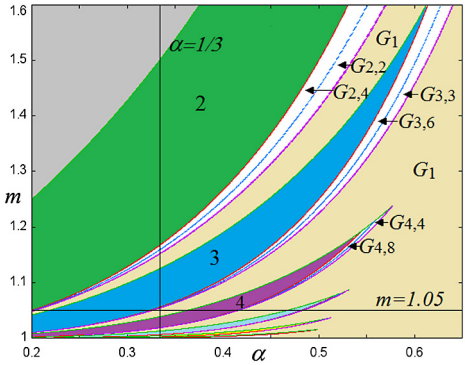

Fig. 10. Bifurcation diagram for Eq. (19) upon Crossing the BC_{LM} curve. This bifurcation diagram is obtained from the bifurcation diagram of the skew-tent map (see Fig. 9), by using Eq. (21). The number, 2, 3, and 4, in the colored areas indicate the periodicity of stable cycles. The yellow region with G_1 indicates a chaotic attractor with one interval. The white regions indicate a chaotic attractor with multiple intervals (the second subscript indicates the number of intervals). With $b < -1$, the Red region for the skew tent map (the region of stable steady state) seen in Fig. 9a would map into Gray in this figure, which is outside of our parameter range. (For interpretation of the references to color in this figure legend, the reader is referred to the web version of this article.)

restrictions. Thus, an immediate transition from the stable steady state $w_L^* = 1$ to an attracting cycle of any period $n \geq 2$, along which the trajectory visits the downward $\boldsymbol{M}$ branch once every n-th period and then visits the upward $\boldsymbol{L}$ branch for $n-1$ consecutive periods, or to a robust chaotic attractor with any number of intervals can occur upon crossing the BC_{LM} curve from **A** to **E-I**. In particular, in the stability region of cycle of period $n \geq 3$ in Fig. 10, the economy converges to an *asymmetric cycle*, along which $n-1$ *consecutive* periods of *gradual* expansion is followed by *one* period of *sharp* downturn, for almost all initial conditions in the neighborhood of the BC_{LM} curve.

The reader might wonder why the periodicity of the stable cycle is higher with a larger α and a smaller m. With a small m, even a small increase in w_t in the downward branch, $w_t \in (1, m)$, causes a sharp increase in the pledgeable rate of return offered by the Bad projects, and hence a sharp increase in the equilibrium rate of return. In addition, a sharper contraction in the Good projects is required to compete with a given increase in the equilibrium rate of return with a larger α. For these reasons, an increase in w_t in the downward branch causes a sharper decline in $w_{t+1} = W(k_{t+1})$ with a larger α and a smaller m. Furthermore, a larger α implies more persistence in the process of capital accumulation, which implies that it takes longer to escape from the upward branch (i.e., it takes time to build up the net worth to the level that enables the agents to finance the Bad projects).

4.4. Inside region ***E-I***[33]

Having seen what happens in **E-I** the moment after crossing the BC_{LM} curve, the reader may wonder what happens as we move away from the BC_{LM} curve and go deeper inside **E-I**. To answer this, we have prepared the two bifurcation diagrams, the one in the $(m, \mu B)$-plane for

[33] Much of this section is based on Section 5 of SGM.

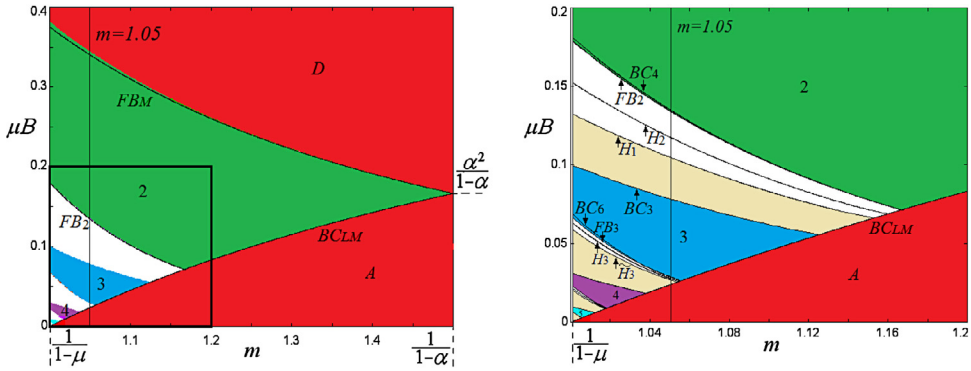

a) $(m, \mu B)$-plane with $\alpha = 1/3$

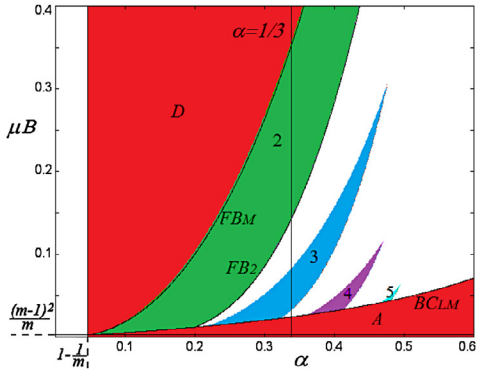

b) $(\alpha, \mu B)$-plane with $m = 1.05$

Fig. 11. Two bifurcation diagrams for Eq. (19): inside region **E-I**.

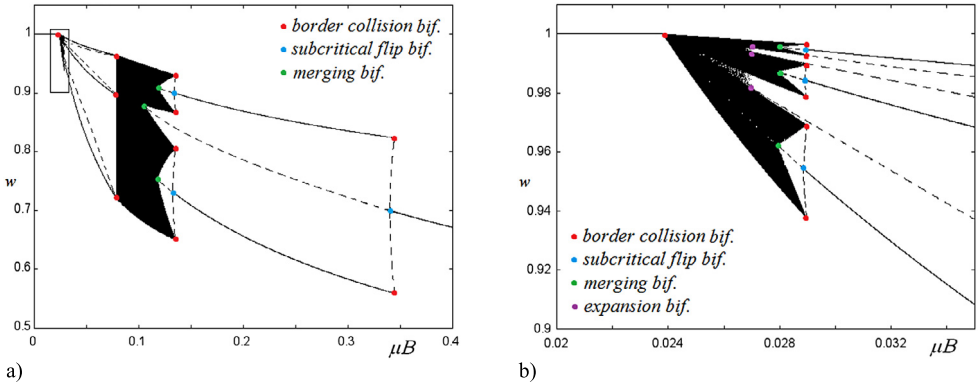

Fig. 12. Effects of μB: a typical bifurcation scenario ($\alpha = 1/3$, $m = 1.05$).

$\alpha = 1/3$ (Fig. 11a, with the right panel showing an enlargement of the boxed area on the left panel) and the other in the $(\alpha, \mu B)$-plane for $m = 1.05$ (Fig. 11b).

For example, for $\alpha = 1/3$, we know that we can find out what happens immediately after crossing the BC_{LM} curve and how it depends on m by tracing the vertical line, $\alpha = 1/3$, in

Fig. 10. This can be also seen by moving along the BC_{LM} curve on Fig. 11a. Likewise, for $m = 1.05$, we know that we can find out what happens immediately after the BC_{LM} curve and how it depends on α by tracing the horizontal line, $m = 1.05$, in Fig. 10. This can be also seen by moving along the BC_{LM} curve on Fig. 11b.

Figs. 11a and 11b further tell us how these parameter regions of various attractors extend into the interior of **E**-**I**, as μB goes up and move away from the BC_{LM} curve. Some of the boundaries of these regions are marked by the types of bifurcations occurring at these boundaries. On the right panel of Fig. 11a, FB_n ($n = 2$ or 3) denotes the lower boundary of the stable n-cycle region, where the stable n-cycle loses its stability due to a *flip bifurcation*; BC_{2n} ($n = 2$ or 3) denotes the *fold BCB* related to subcritical FB_n; BC_3 denotes the upper boundary of the stable 3-cycle region, where the stable 3-cycle disappears due to a *fold BCB*; H_n ($n = 1, 2$ or 3) denotes the boundary between $G_{n,2n}$ and $G_{n,n}$ due to a *merging bifurcation* (i.e., a pairwise merging of chaotic intervals, caused by the *homoclinic bifurcation* of a unstable cycle with negative eigenvalue); $\tilde{H}_3$ denotes the boundary between $G_{3,3}$ and G_1 due to an *expansion bifurcation* (i.e., a discontinuous increase in the size of the chaotic attractor, caused by the *homoclinic bifurcation* of a unstable cycle with positive eigenvalue). See SGM for the derivation of the analytical conditions for these bifurcation curves.

Although this may not be visible in Figs. 11a and 11b, some of these parameter regions can overlap, which means a co-existence of a pair of attractors (due to the occurrence of subcritical bifurcations). To be able to see it more clearly, we have prepared Fig. 12a (with Fig. 12b showing an enlargement of the boxed area in Fig. 12a), in which the attractors (and some of the unstable cycles and the unstable steady state) are plotted against μB for $\alpha = 1/3$ and $m = 1.05$. Figs. 12 thus show a bifurcation sequence, as we move along the vertical line, $m = 1.05$, in Fig. 11a, or equivalently, the vertical line, $\alpha = 1/3$, in Fig. 11b. We have chosen $\alpha = 1/3$ and $m = 1.05$ because this bifurcation diagram displays all different types of bifurcations discussed in a single sequence.

Let us start in **D** with a high μB. As seen in Fig. 12a, decreasing μB first leads to a fold BCB, which creates the stable 2-cycle. This co-exists with the stable steady state, until it becomes unstable via a subcritical flip bifurcation, as we enter **E**-**I**, after which the stable 2-cycle is the only attractor. Then, another BCB creates a chaotic attractor with 4 intervals. This co-exists with the stable 2-cycle, until it becomes unstable in a subcritical flip. Then, the chaotic attractor with 4 intervals experiences a pairwise merging to become a chaotic attractor with 2 intervals via a merging bifurcation (where the unstable 2-cycle is seen colliding with the merging intervals via a homoclinic bifurcation). The chaotic attractor with 2 intervals then becomes a chaotic attractor with a single interval (where the unstable steady state is seen colliding with the merging intervals via a homoclinic bifurcation). Then, the chaotic attractor with a single interval disappears and a pair of 3-cycles, one stable and one unstable, is born via a fold BCB. After this, the stable 3-cycle is the only attractor, until (now moving to Fig. 12b), a BCB creates a chaotic attractor with 6 intervals, which co-exist with the stable 3-cycle until the latter becomes unstable in a subcritical flip. Then, the chaotic attractor with 6 intervals experiences with a pairwise merging to become a chaotic attractor with 3 intervals (where the unstable 3-cycle born at the subcritical flip is seen colliding with the merging intervals via a homoclinic bifurcation). Then, the chaotic attractor with 3 intervals experiences a discontinuous increase in its size via an expansion bifurcation to become a chaotic attractor with one interval (where the unstable 3-cycle born at a fold BCB is seen colliding with the chaotic attractor via a homoclinic bifurcation). After this, the chaotic attractor with one interval is the unique attractor, which continuously shrinks its size and

disappears upon entering Region **A**. We summarize this bifurcation sequence schematically as follows:

$$w_M^* \overset{BC_2}{\Rightarrow} \{w_M^*, 2\} \overset{FB_M}{\Rightarrow} 2 \overset{BC_4}{\Rightarrow} \{2, G_{2,4}\} \overset{FB_2}{\Rightarrow} G_{2,4} \overset{H_2}{\Rightarrow} G_{2,2} \overset{H_1}{\Rightarrow} G_1 \overset{BC_3}{\Rightarrow} 3 \overset{BC_6}{\Rightarrow} \{3, G_{3,6}\}$$
$$\overset{FB_3}{\Rightarrow} G_{3,6} \overset{H_3}{\Rightarrow} G_{3,3} \overset{\tilde{H}_3}{\Rightarrow} G_1 \overset{BC_{LM}}{\Rightarrow} w_L^*.$$

Finally, let us end our discussion of the interior of **E-I** region with some numerical plots of the equilibrium trajectories to see what happens during the transient phase (Figs. 13). Again, we have set $\alpha = 1/3$ and $m = 1.05$ and chosen values of μB from each of the parameter regions discussed above. Although we have chosen the initial condition fairly close to its attractor, these plots show that the convergence to the attractor is not immediate. Indeed, this model is capable of generating quite irregular fluctuations during the transient phase even in the parameter regions of stable cycles. For example, Fig. 13e shows the case where the equilibrium trajectory asymptotically converges to a stable 3-cycle. This plot shows that during the transient phase, the equilibrium trajectory looks more like an irregular 6-cycle, and to the naked eye, it is hardly distinguishable from the case of chaotic attractors with 6 intervals, illustrated in Fig. 13f. Yet, the asymmetry of fluctuations, the patterns of "up", "up," "down," "up", "up," and "down," can be seen clearly, which is what one should expect from our result in Section 4.3 that, upon crossing the BC_{LM} curve, the economy experiences two periods of expansion followed by one period of downturn along its only stable 3-cycle.

5. Concluding remarks

This paper studied a dynamic general equilibrium model with financial frictions, in which the economy fluctuates endogenously along its unique equilibrium trajectory. What generates fluctuations is the changing composition of credit flows across heterogeneous investment projects, which we call the *Good* and the *Bad*. The Good require the inputs supplied by others. By generating demand for them, they improve net worth of other borrowers. The Bad are independently profitable, so that they generate less demand spillovers than the Good. Furthermore, the Bad are subject to the borrowing constraint so that the agents need to have a high level of net worth to be able to initiate the Bad projects. When the net worth is low, the agents cannot finance the Bad, and all the credit goes to the Good, even when the Bad are more profitable than the Good. This over-investment to the Good creates a boom, leading to an improved net worth. The agents are now able to invest into the Bad. This shift in the composition of the credit from the Good to the Bad at the peak of the boom causes a decline in net worth. The whole process repeats itself. Endogenous fluctuations occur because the Good breed the Bad and the Bad destroy the Good. Such instability and persistent volatility occur when the following two conditions hold. First, the Bad projects need to be highly profitable so that the agents are always eager to run them. Second, the Bad projects come with an intermediate degree of pledgeability, so that the agents cannot finance them when their net worth are low, but they can when their net worth are high. This implies, among other things, that an improvement in the financial system could lead to more volatility.

Although this mechanism was already discussed in Matsuyama (2013, Sections 2–4), many additional ingredients of the model, which were introduced to demonstrate the robustness of the mechanism and to clarify the assumptions that are essential from those that are merely simplifying, had unfortunately ended up obscuring the mechanism. In this paper, we have shown that the same dynamical system that governs the equilibrium trajectory can be obtained by a much

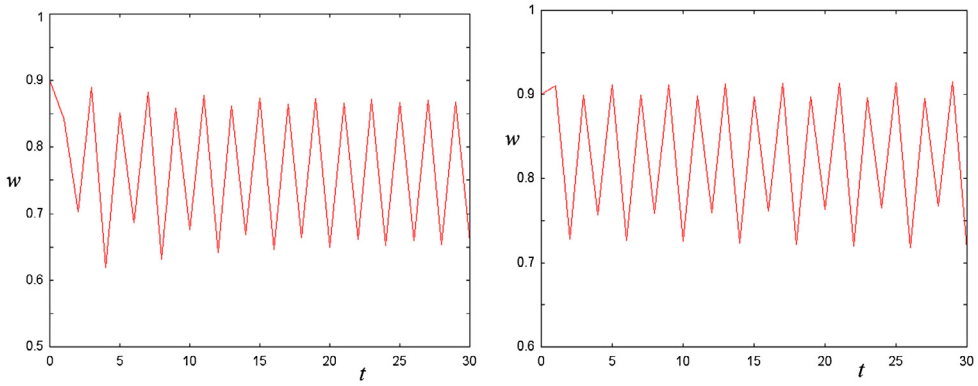

a) μB=0.2 (2-cycle), with $w_0 = 0.9$.

b) $\mu B = 0.125$ ($G_{2,4}$), with $w_0 = 0.9$.

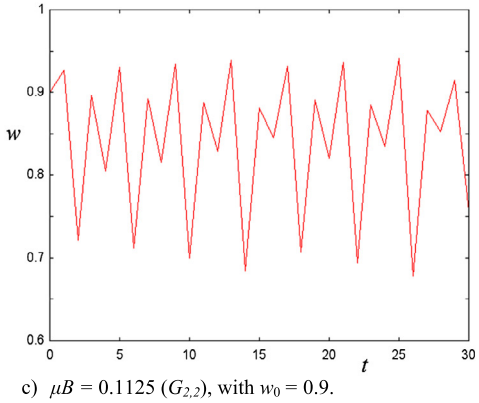

c) $\mu B = 0.1125$ ($G_{2,2}$), with $w_0 = 0.9$.

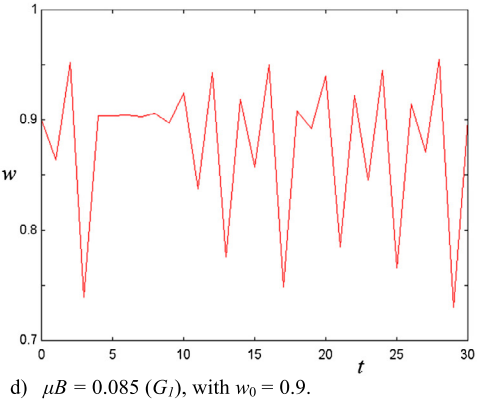

d) $\mu B = 0.085$ (G_1), with $w_0 = 0.9$.

Fig. 13. Some trajectories ($\alpha = 1/3$, $m = 1.05$).

simpler setting, which should help to highlight the mechanism through which financial frictions cause instability and persistent fluctuations. It should also help to make this model more useful as a building block for future research.

Furthermore, we discussed in greater detail the nature of fluctuations observed for the case where the production of the final good is Cobb–Douglas. For example, the unique steady state possesses the *corridor stability*, which means that it is locally stable but globally unstable. This also suggests that, when a parameter change causes its local stability, the effects are *catastrophic* and *irreversible*. Furthermore, the dynamics may be characterized by an *immediate* transition from the stable steady state to a stable *asymmetric cycle* of period $n \geq 3$, along which $n - 1 \geq 2$ consecutive periods of gradual expansion are followed by one period of sharp downturn, or by an *immediate* transition to *robust chaotic attractors*. We are able to show these results thanks to recent advances in the theory of piecewise smooth (i.e., regime-switching) dynamical systems, which have many properties that are quite distinct from and much simpler than those defined by smooth dynamical systems. In particular, we demonstrated how the skew-tent map provides a powerful tool for characterizing a regime-switching system. Although a rigorous presentation of these tools was well beyond the scope of this paper, we have strived to make it accessible to the economics audience. We hope that our non-technical, heuristic exposition, and "cookbook" presentation of how to use it, written in the economist-friendly language, serves as an introduction to

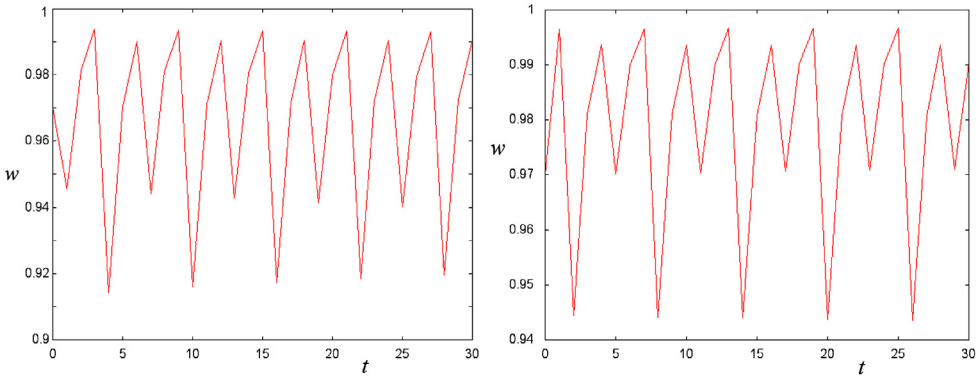

e) $\mu B = 0.032$ (3cycle), with $w_0 = 0.97$.

f) $\mu B = 0.0285$ ($G_{3,6}$), with $w_0 = 0.97$.

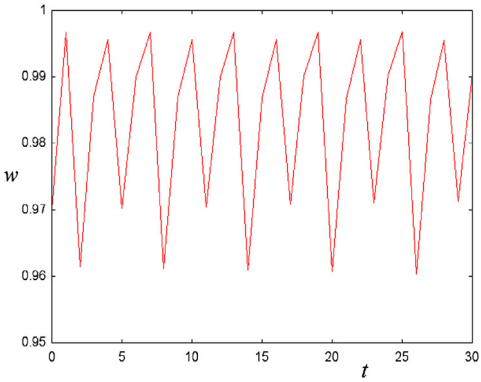

g) $\mu B = 0.0275$ ($G_{3,3}$), with $w_0 = 0.97$.

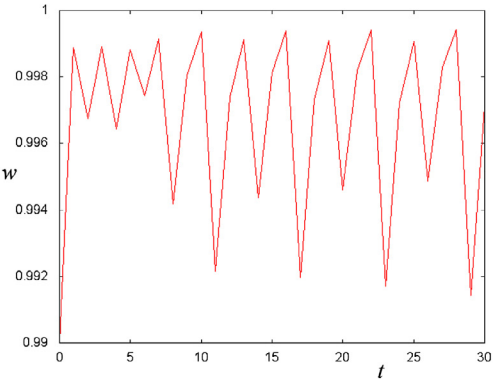

h) $\mu B = 0.0245$ (G_1), with $w_0 = 0.99$.

Fig. 13. (*continued*)

this branch of mathematics, which should provide powerful tools for analyzing regime-switching nonlinear dynamic economic models.

References

Aghion, Philippe, Abhijit, Banerjee, Piketty, Thomas, 1999. Dualism and macroeconomic volatility. Q. J. Econ. 114 (4), 1359–1397.

Avrutin, Viktor, Laura Gardini, Michael Schanz, Iryna Sushko, Fabio Tramontana, 2015. Continuous and Discontinuous Piecewise-Smooth One-Dimensional Maps: Invariant Sets and Bifurcation Structure, World Scientific. Book manuscript dated on April 28, 2015.

Azariadis, Costas, Smith, Bruce D., 1998. Financial intermediation and regime switching in business cycles. Am. Econ. Rev. 88 (3), 516–536.

Baumol, William J., Benhabib, Jess, 1989. Chaos: significance, mechanism, and economic applications. J. Econ. Perspect. 3, 77–105.

Benhabib, Jess, Miyao, Takahiro, 1981. Some new results on the dynamics of the generalized Tobin model. Int. Econ. Rev. 22, 589–596.

Bernanke, Ben, Gertler, Mark, 1989. Agency costs, net worth, and business fluctuations. Am. Econ. Rev. 79, 14–31.

Diamond, Peter, 1965. Government debt in a neoclassical growth model. Am. Econ. Rev. 55, 1126–1150.

Favara, Giovanni, 2012. Agency problems and endogenous investment fluctuations. Rev. Financ. Stud. 25 (7), 2301–2342.

Figueroa, Nicolás, Leukhina, Oksana, 2013. Liquidity and credit cycles. Working Paper. University of Washington.

Gardini, Laura, Sushko, Iryna, Naimzada, Ahmad K., 2008. Growing through chaotic intervals. J. Econ. Theory 143, 541–557.
Kindleberger, Charles P., 1996. Manias, Panics, and Crashes: A History of Financial Crises, third edition. John Wiley & Sons, Inc., New York.
Kiyotaki, Nobuhiro, Moore, John H., 1997. Credit cycles. J. Polit. Econ. 105, 211–248.
Leijonhufvud, Axel, 1973. Effective demand failures. Swed. J. Econ., 27–48.
Martin, Alberto, 2008. Endogenous credit cycles. Working Paper. CREI and Universitat Pompeu Fabra.
Matsuyama, Kiminori, 1999. Growing through cycles. Econometrica 67, 335–347.
Matsuyama, Kiminori, 2007. Credit traps and credit cycles. Am. Econ. Rev. 97, 503–516.
Matsuyama, Kiminori, 2008. Aggregate implications of credit market imperfections. In: Acemoglu, D., Rogoff, K., Woodford, M. (Eds.), NBER Macroeconomics Annual 2007. In: NBER Book Series NBER Macroeconomics Annual, vol. 22. University of Chicago Press, pp. 1–60.
Matsuyama, Kiminori, 2013. The good, the bad, and the ugly: an inquiry into the causes and nature of credit cycles. Theor. Econ. 8, 623–651.
Mendoza, Enrique G., Terrones, Marco E., 2008. An anatomy of credit booms: evidence from macro aggregates and micro data. NBER Working Paper, 14049.
Minsky, Hyman P., 1982. The financial instability hypothesis: capitalistic processes and the behavior of the economy. In: Kindleberger, C.P., Laffargue, J.P. (Eds.), Financial Crises: Theory, History, and Policy. Cambridge University Press, Cambridge, pp. 13–29.
Myerson, Roger B., 2012. A model of moral hazard credit cycles. J. Polit. Econ. 105, 847–878.
Myerson, Roger B., 2014. Moral-hazard credit cycles with risk-averse agents. J. Econ. Theory 153, 74–102.
Reichlin, Pietro, Siconolfi, Paolo, 2004. Optimal debt contracts and moral hazard along the business cycle. Econ. Theory 24, 75–109.
Schularick, Moritz, Taylor, Alan M., 2012. Credit booms gone bust: monetary policy, leverage cycles, and financial crises, 1870–2008. Am. Econ. Rev. 102 (2), 1029–1061.
Sushko, Iryna, Avrutin, Viktor, Gardini, Laura, 2015. Bifurcation structure in the skew tent map and its application as a border collision normal form. J. Differ. Equ. Appl., 1–48.
Sushko, Iryna, Gardini, Laura, Matsuyama, Kiminori, 2014a. Superstable credit cycles and U-sequence. Chaos Solitons Fractals 59, 13–27.
Sushko, Iryna, Gardini, Laura, Matsuyama, Kiminori, 2014b. Chaos in a model of credit cycles with good and bad projects. WP-EMS #2014/05. University of Urbino, downloadable at: http://www.econ.uniurb.it/RePEc/urb/wpaper/WP_14_05.pdf.
Tirole, Jean, 2005. The Theory of Corporate Finance. Princeton University Press, Princeton.